Journal of Volcanology and Geothermal Research 446 (2024) 107996

Contents lists available at ScienceDirect

Journal of Volcanology and Geothermal Research

journal homepage: www.journals.elsevier.com/journal-of-volcanology-and-geothermal-research

Compositional variations in shield-stage volcanism in Fogo, Cape Verde islands

Brendon Rolfe-Betts [a], Simon J. Day [b], Hilary Downes [a,c,*], Ian Millar [d], Kristina Palubicki [a,c]

[a] School of Natural Sciences, Birkbeck University of London, Malet Street, London WC1E 7HX, UK
[b] Institute for Risk and Disaster Reduction, University College London, Gower Street, London WC1E 7HX, UK
[c] Department of Earth Sciences, Natural History Museum, Cromwell Rd, London, UK
[d] NERC Environmental Isotope Facility, Keyworth, UK

ARTICLE INFO

Keywords:
Volcano collapse
Lava compositions
Fractional crystallization
Radiogenic isotopes
Assimilation
Carbonatites

ABSTRACT

The intraplate oceanic island of Fogo (Cape Verde islands) is in the shield-stage of its evolution. It experienced a major lateral collapse ca. 70 ka ago, after which a sequence of lavas about 2 km thick infilled the collapse scar, with eruptions continuing to the present day. Nearly 100 lavas from before and after the collapse have been sampled and analysed for bulk rock compositions. These lavas have been divided into five Formations (2 pre-collapse and 3 post-collapse), using stratigraphic principles. There is little difference in the major and trace element compositions of pre- and post-collapse lavas, and the main process that gives rise to their diversity is fractional crystallization of observed mineral phases. Pre-collapse lavas show a narrower range of bulk compositions than the post-collapse lavas, but this may be because the sampling strategy avoided these more altered and poorly exposed lavas. A group of high-P_2O_5 lavas, erupted both before and after the collapse, may have been extensively contaminated by local seamount-stage intrusive carbonatites. A subset of 30 samples was analysed for Sr, Nd and Pb isotope ratios. They show a plume component which has interacted with two contaminants: (1) an increase in $^{87}Sr/^{86}Sr$ and decrease in $^{143}Nd/^{144}Nd$ with decreasing MgO, which indicates varying amounts of assimilation of an enriched lithospheric component coupled to fractionation (AFC), and (2) contamination of the more fractionated magmas, without further fractionation, involving the suspected carbonatite contaminant which originates from a more isotopically depleted source. Overall trends of increasing $^{87}Sr/^{86}Sr$, and slight decreases in $^{143}Nd/^{144}Nd$ and all radiogenic Pb isotope ratios, with decreasing age of eruption, indicate a general increase in the assimilated lithospheric component throughout shield-stage activity. However, there is no clear evidence of any change in isotope compositions across the period of the collapse. All Formations show similar wide and overlapping ranges of isotope compositions, regardless of the timescales represented by each Formation. This implies that much short-term variation in the magma sources was superimposed on the overall trend of increasing lithospheric assimilation.

1. Magmatism in Fogo

1.1. Eruptive sequences and formation-level stratigraphic units

The island of Fogo in the Cape Verde archipelago (Fig. 1) is an intraplate oceanic island in the sub-aerial shield-stage of volcanic activity (Day et al., 1999). Dating of exposed rocks shows that this shield-stage volcanism started at least 160 ka ago (Cornu et al., 2021) and continues to the present, with the most recent eruption in 2014–15. Early attempts to define the history of the Fogo volcano interpreted it in terms of initial growth of a low-angle shield volcano dominated by mafic lavas, followed by growth of a steeper-sided central stratovolcano with a greater proportion of pyroclastic rocks (Machado and Torre de Assuncao, 1965; Machado and Torre de Assuncao, 1965). This central volcano then experienced vertical collapse of a summit caldera followed by growth of a new central cone – the Pico do Fogo – within the caldera. The lack of an eastern caldera wall was attributed to large-scale regional faulting (Machado and Torre de Assuncao, 1965). Some subsequent studies (Brum da Silveira et al., 1995, Brum da Silveira et al., 1997a, 1997b; Torres et al., 1998; Madeira1a et al., 2005; Martínez-Moreno et al., 2018) have retained this interpretation, despite the lack of outcrop evidence for such regional faults offsetting pre-collapse sequences

* Corresponding author at: School of Natural Sciences, Birkbeck University of London, Malet Street, London WC1E 7HX, UK.
E-mail address: h.downes@bbk.ac.uk (H. Downes).

https://doi.org/10.1016/j.jvolgeores.2023.107996
Received 29 July 2023; Received in revised form 24 December 2023; Accepted 27 December 2023
Available online 11 January 2024

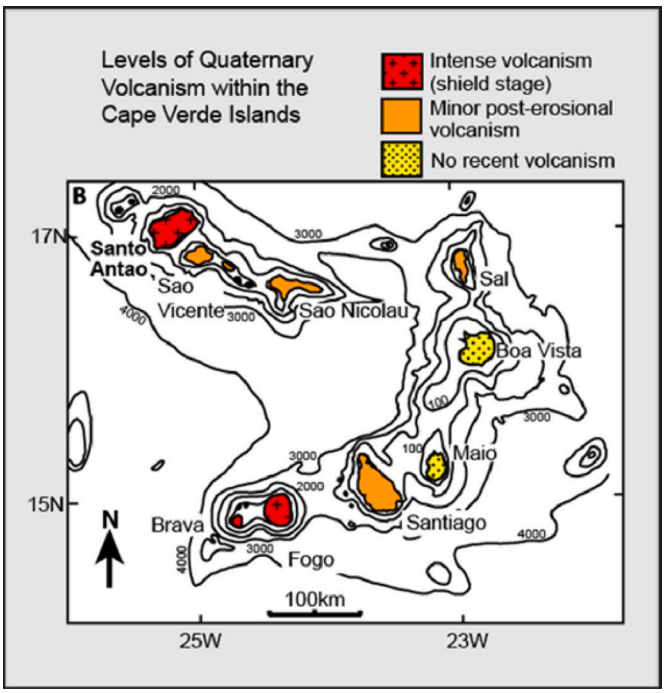

Fig. 1. Location of island of Fogo in Cape Verde Archipelago (modified after Day et al., 1999).

exposed in the eastern part of the island.

The alternative interpretation of the history and structure of Fogo was first proposed by Day et al. (1999). This considered that a giant eastward-directed sector collapse, the Monte Amarelo collapse, removed the old summit and much of the east side of the island. This interpretation is supported by mapping of large-volume debris avalanche and debris flow deposits offshore (Le Bas et al., 2007; Masson et al., 2008; Barrett et al., 2020) and by the discovery of deposits from giant tsunami waves onshore on the adjacent islands of Santiago and Maio (Paris et al., 2011; Ramalho et al., 2015; Madeira et al., 2020). Absolute dating has placed the Monte Amarelo collapse at ~70 ka ago (Paris et al., 2011; Ramalho et al., 2015; Maccaferri et al., 2017; Cornu et al., 2021). Some uncertainty remains about the age of collapse and also the possibility that more than one landslide may have occurred (Marques et al., 2019), but here we follow the single sector collapse interpretation of Day et al. (1999).

The Monte Amarelo collapse is a key marker in the shield-stage history of Fogo that divides the rock sequences into older pre-collapse and younger post-collapse units. Such a simple two-fold division has limitations when considering patterns of compositional variation in sequences of lavas erupted over shorter time intervals. Nevertheless, it has been used as a division with which to investigate temporal compositional variations in Fogo magmas (Cornu et al., 2021; Lo Forte et al., 2023).

The present study has used the work of Day et al. (1999) and an unpublished geological map of the island by SJD to provide insight into the evolution of Fogo before and after the Monte Amarelo collapse (Fig. 2; Table 1). The aims of our study were to understand the petrogenesis of the lavas, and to investigate whether there are any significant differences between the compositions of lavas erupted before and after the collapse. Such differences are seen in other volcanic edifices reviewed by Watt (2019) that are greater than, or different in nature from, compositional differences developed over shorter time intervals within both pre- and post-collapse periods.

The limited outcrops of oldest sub-aerial lavas (the Monte Barro Group; Table 1) were not sampled for this study because of their pervasive alteration. We also did not sample the still older Ribeira Almada Group (Table 1) which consists mainly of plutonic carbonatites cut by alkaline mafic silicate dikes, with one outcrop of heavily altered mafic silicate rocks that may be of submarine volcanic origin. Age data (Hoernle et al., 2002) indicate that these are much older than the shield-stage rocks of Fogo. Instead, this study focuses on the mainly mafic lavas that, together with subordinate scoria, lapilli and epiclastic sediments, form the main shield-stage sequences.

Our oldest samples are from the Bordeira Formation (Table 1), which forms most of the pre-collapse Monte Amarelo shield volcano. Outcrops of Bordeira Formation lavas can be found in deeply incised dry river channels (ribeiras) on the outer slopes of the Monte Amarelo volcano around the island, and in the Bordeira cliff which is the main exposed part of the eroded collapse scar. These lavas are thought to have been erupted from a series of three volcanic centres aligned on a N-S trend but each with its own triple-armed radial dike swarms (Fig. 2a; Day et al., 1999). They vary from aphyric to moderately porphyritic (25%), but a small proportion are highly olivine- and/or clinopyroxene-phyric. Where outcrop is poor or limited in vertical extent, this can cause local ambiguities as to whether particular highly porphyritic flows belong to the Bordeira Formation or to the overlying Ribeira Aguadinha Formation, which is distinguished by its high phenocryst content as discussed below.

The Bordeira Formation is overlain by the Ribeira Aguadinha Formation (Fig. 2b), the remains of which are found mostly in the east of the island where it is up to a few hundred metres thick (Fig. 2b). It occurs more widely at or very near the top of the sequences exposed in the Bordeira cliff and as a thinner (typically a few tens of metres or less thick) and more discontinuous unit on the southern and western slopes of Fogo. These slopes have been incised by many small ribeiras, so that the outcrop patterns of the Bordeira and Ribeira Aguadinha Formations are extremely complex and can only be accurately represented on a large geological map. We emphasize that Fig. 2 should only be regarded as a broad guide to the geology of Fogo.

The Ribeira Aguadinha Formation lavas are associated with a distinct mainly N-S aligned dike swarm, cross-cutting the earlier radial dike swarms, whose emplacement immediately preceded the Monte Amarelo collapse (Day et al., 1999). Both the late N-S dikes and the lavas of the Ribeira Aguadinha Formation are characterized by unusually high contents of pyroxene phenocrysts (up to 45%) compared to the older dikes and lavas, and by the distinctive dark, purple-brown surface weathering of the groundmass. This “ankaramitic” appearance is seen in all these late pre-collapse lavas and associated dikes, with only one exception within the sequence of otherwise “ankaramitic” lavas. The exception is a sparsely pyroxene-phyric lava that does, however, include strongly pyroxene-rich enclaves. These “ankaramites” therefore form strong evidence of a petrological (but not geochemical) change in erupted magmas before the collapse, at the boundary between the generally less phenocryst-rich Bordeira and the almost entirely “ankaramitic” Ribeira Aguadinha Formations.

The oldest post-collapse unit identified in this study is the Monte Duarte Formation (Table 1, Fig. 2c). It is defined as being composed of (i) a sequence of lavas buried within the collapse scar, perhaps as much as 2 km thick but not accessible for sampling in surface outcrop, and (ii) a thin (typically less than tens of metres thick) and discontinuous sequence on the slopes of Fogo outside the collapse scar, erupted from monogenetic flank vents and also incised by ribeiras. The latter provided most of the outcrops of Monte Duarte Formation rocks that we sampled. A few corresponding lava flows occur upslope at the Bordeira cliff, where they outcrop overlying the Ribeira Aguadinha Formation “ankaramitic” lavas at the top of the cliff and truncated by it. These lavas are interpreted as the product of post-collapse vents on the rim of the collapse scar which have since been removed by post-collapse retreat of the cliff. The end of the Monte Duarte Formation is defined by the end of flank eruptions in W and SW Fogo (Foeken et al., 2009), and by the first occurrence of preserved lava platforms at the coast.

In contrast to the wide distribution of Monte Duarte Formation rocks,

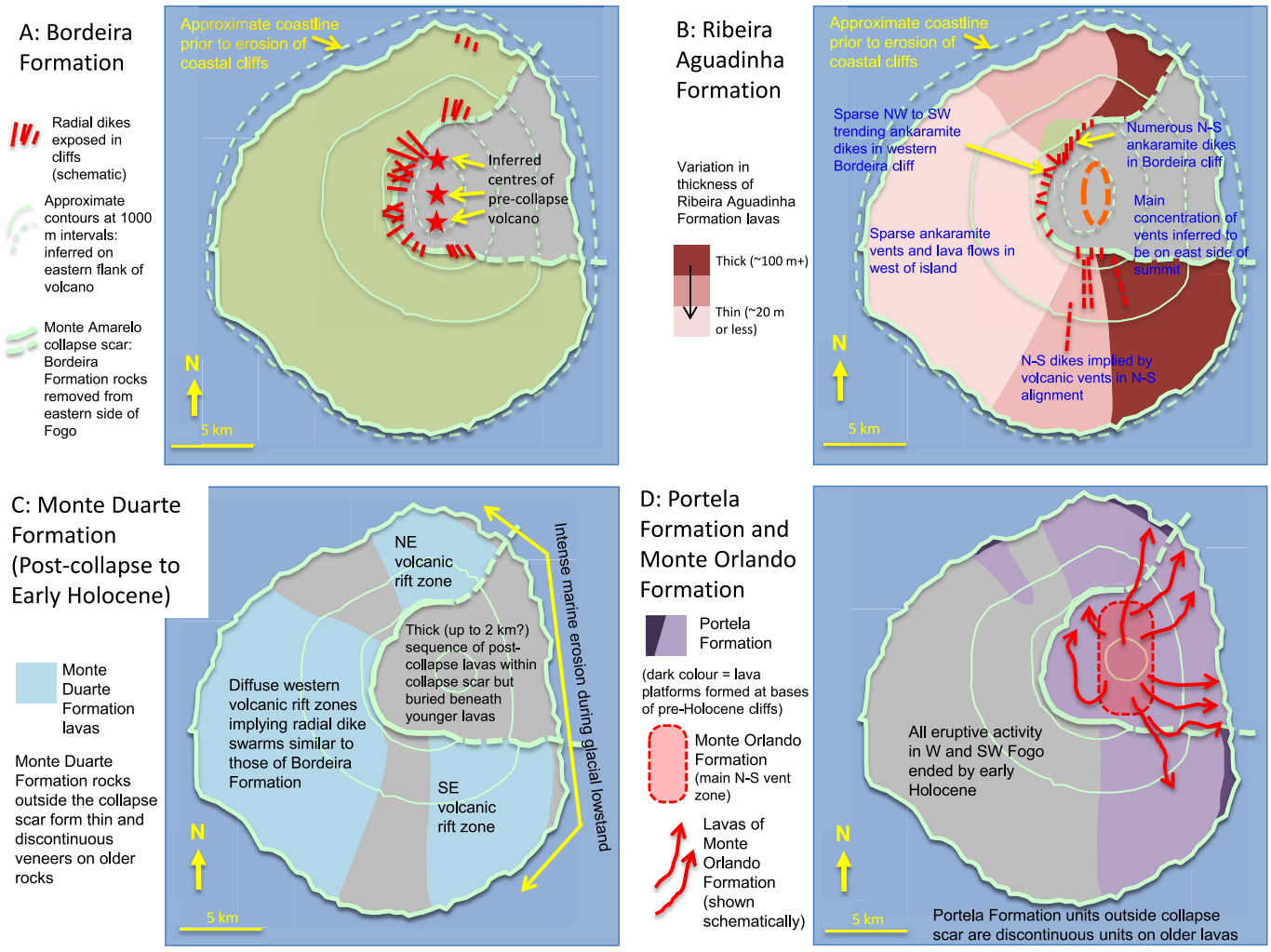

Fig. 2. Geological history of the shield-stage eruptions of Fogo, Cape Verdes, modified after Day et al. (1999). Panels (A) and (B) show eruptions before the Monte Amarelo collapse, whereas panels (C) and (D) show post-collapse eruptions.

the later post-collapse lava flows occur almost entirely in the east of the island, forming the Portela and Monte Orlando Formations (Table 1; Fig. 2d). Portela Formation lavas were mainly erupted from the summit of the Pico do Fogo and from flank vents in volcanic rift zones extending NNE and SE to the coast outside the collapse scar. The Monte Orlando Formation activity began with the end of intense summit activity at the Pico do Fogo and development of a new N-S aligned vent zone to the west and at the foot of the Pico do Fogo (Day et al., 1999). This activity continues to the present-day, and lavas of all recent eruptions (i.e., those since 1785) form part of the Monte Orlando formation.

The use of this stratigraphic scheme of five Formations to subdivide the shield-stage rocks of Fogo presents a problem in relating our analyses to data sets from previous studies that have not used this scheme. However, this can be addressed in most cases by examining the sampling strategies in published works. This has enabled us to compare our new data with data sets from at least some previous studies.

Most studies that investigated the older shield-stage rocks on Fogo involve samples collected from the foot of the Bordeira cliff or, in the case of Cornu et al. (2021), samples collected in near-vertical traverses up the cliff. These samples, except for those from the very top of the cliff, can be confidently assigned to the pre-collapse sequence, although it is not always possible to assign them to the Bordeira or Ribeira Aguadinha Formations. In other studies that have collected samples of older rocks from road traverses up the coastal cliffs of Fogo are more problematic, and in those that do not provide detailed location information we were unable to assign the samples to pre- or post-collapse ages. Very few studies have collected samples from inland areas on the slopes of Fogo outside the collapse scar, except those carried out with help from SJD and that use an earlier version of this stratigraphy (e.g., Foeken et al., 2009, 2012; Hildner et al., 2012). As a result, many previous studies tend to have a large gap between samples of pre-collapse lavas and samples from the most recent Formations, with few or no samples from our earlier post-collapse Formations. This gap in sampling is problematic, but the complexity of outcrop patterns on these slopes means that it would be hard for us to assign older post-collapse samples from these studies to one or another of our Formations.

Studies of the younger rocks of Fogo have tended to focus on historic eruptions of known dates, which we have assigned to the Portela (pre-1785 eruptions) and Monte Orlando (1785 and later) Formations. Some of these studies have analysed lavas from the most recent eruptions, with sufficiently large sample sets that enable examination of intra-eruption compositional variations (e.g., Barker et al., 2023). Various aspects of the petrology, geochemistry and geothermobarometry of the rocks from the eruptions of 1951, 1995 and 2014–15 have been investigated by Hildner et al. (2011, 2012); Mata et al. (2017) and Klügel et al. (2020). The latter used a subset of the samples from the 2014–15 eruption that were collected by us; bulk rock analyses of the complete set of these samples are presented in this paper.

Table 1
Simplified stratigraphy of island of Fogo (after Day et al., 1999).

Cha das Caldeiras Group	**Monte Orlando Formation**	**All historic lavas since 1785 BCE Erupted from vents within collapse scar, mainly on N-S fissure trends**
	End of summit eruptions from Pico do Fogo (18th Century)	
	Portela Formation	**Continued intense eruptive activity within the collapse scar Scattered lavas outside collapse scar from vents on NE and SW rifts**
	End of coastal cliff formation (early Holocene?) and cessation of eruptions in SW of Fogo (~9 ka)	
	Monte Duarte Formation	**Thick sequence of lavas within collapse scar (earliest post-collapse rocks poorly exposed). Varied lavas forming thin veneer outside collapse scar**
	Monte Amarelo lateral collapse	
Monte Amarelo Group	**Ribeira Aguadinha Formation**	**Strongly pyroxene-phyric lavas erupted from vents on dominant N-S dike swarm**
	Structural reconfiguration of Monte Amarelo volcano	
	Bordeira Formation	**Lavas erupted from three overlapping volcanic centres each with radial dike swarms**
Major unconformity – valley incision and coastal erosion		
Monte Barro Group (earliest subaerial lavas)		
Major unconformity – emergence of island		
Ribeira de Almada Group (alkali basic seamount series with carbonatite intrusions)		

Samples in this study have been collected from the pre-collapse Bordeira and Ribeira Aguadinha Formations, and from the post-collapse Monte Duarte, Portela and Monte Orlando Formations, which includes the most recent (2014–15) eruption.

1.2. Age ranges of the five formations and potential patterns of isotopic variation

The age ranges represented by each of the five Formations (Table 1) can be defined by the existing radiometric age data, Cosmic Ray Exposure (CRE) data and stratigraphic constraints (Day et al., 1999). The oldest exposed rocks from the Bordeira Formation dated by Cornu et al. (2021) are in the range 160–120 ka. Altered parts of the Bordeira Formation, exposed as much as 1 km below its top surface in the lowest parts of the Bordeira cliff and in coastal cliffs, are likely to be much older but remain undated. Since the Ribeira Aguadinha Formation is less than a tenth of the thickness of the Bordeira Formation, it may represent a much shorter time period of activity, perhaps as little as 10 ka if a similar eruption rate is assumed. The Ribeira Aguadinha Formation was terminated by the Monte Amarelo collapse (ca. 70 ka, according to Cornu et al., 2021). However, highly porphyritic lavas from the very top of the pre-collapse sequence with preserved flow tops were dated using the CRE method by Foeken et al. (2009, 2012) and in one case gave a surprisingly old age of 126 ka that was subsequently confirmed by Ar-Ar dating (Foeken et al., 2012). This may be explained if this flow (sample FG15RB15), in the extreme south west of Fogo, is one of the rare extremely porphyritic lavas within the Bordeira Formation rather than belonging to the "ankaramitic" Ribeira Aguadinha Formation. This anomaly points to strong lateral variations in eruption rates, over time, between the three volcanic centres shown in Fig. 2a. Detailed examination of this topic must await publication of the geological map by SJD, but we discuss implications of possible wide spatial and temporal variations for the choice of sampling strategy further below.

The Monte Duarte Formation consists of lavas erupted in a period from the time of the Monte Amarelo collapse to the end of eruptions in the west of the island around 9 ka ago, based on CRE dating of the youngest eruptions there (Foeken et al., 2009). This is also the time when lava platform formation began, mainly in the east of Fogo, in the early Holocene when sea levels stabilized close to present-day values (Day et al., 1999). This age is constrained by using the same interpretation of coastal cliff, scree and lava platform formation sequences as applied to Canary Island shield-stage volcanoes by Guillou et al. (1998) and Carracedo et al. (1999, 2001). Therefore, the duration of the Monte Amarelo Formation is around 60 ka, similar to the duration of the dated part of the Bordeira Formation.

The Portela Formation (Table 1) runs from the early Holocene (platform-forming) lavas through to the end of intense summit activity of the Pico do Fogo in the early 18th Century. We used mapping that defines the early platform-forming lavas and younger prehistoric lavas, and flow-by flow mapping of the youngest lavas, in conjunction with various historic accounts collected by Ribeiro (1960) and analysed in Day et al. (2000). The Portela Formation has a duration of approximately 10 ka, comparable to that inferred for the Ribeira Aguadinha Formation. The Monte Orlando Formation consists of those lavas erupted after the end of summit activity, from fissures aligned roughly along a new N-S trend (Day et al., 1999), and therefore has a duration of only about 300 years.

The wide spread in inferred durations of these five formally defined Formations, by more than two orders of magnitude from a few hundred years (Monte Orlando Formation) through around 10 ka (Ribeira Aguadinha Formation and Portela Formation), to several tens of thousands of years (sampled part of Bordeira Formation; and the whole of the Monte Duarte Formation) has a useful consequence. It becomes possible to gain insight into the timescales over which variations in magma source compositions are expressed in the isotope compositions of the erupted lavas. At one extreme, if the magma supply was of uniform isotope composition at any one time but varied through time over the whole sampled history of Fogo, then we should expect to see different mean isotopic compositions for each Formation and little overlap in the distributions of individual sample compositions between Formations. At another extreme, if the compositions of magma supply varied cyclically or randomly on timescales shorter than the durations of at least some of the Formations, then there should be much more overlap in the isotopic ranges of lavas of those Formations. If the timescales of compositional variation were only longer than the shorter durations of some Formations, then those Formations should show more limited isotopic ranges than those shown by the Formations with longer durations. These potential patterns of isotopic variation with time will be compared against the observed patterns described later.

1.3. Crust and lithosphere beneath Fogo Island

Other than very limited outcrops of the Ribeira de Almada Group (Table 1), there is only indirect evidence for the compositions of the older rocks through which the shield-stage lavas of Fogo were erupted. These rocks could include the oceanic mantle lithosphere and the Mesozoic oceanic crust, but also pre-shield-stage rocks associated with the early growth of the Fogo volcanic edifice. The latter may include both seamount-stage submarine volcanic rocks and intrusions of alkaline magmas emplaced into any or all of these older units, at depths ranging from within the edifice to the sub-crustal lithosphere. Three sources of information enable us to establish the nature of the rocks through which Fogo magmas have passed and therefore the nature of potential contaminants: (1) the abundant xenoliths brought to the surface by the erupting alkaline magmas; (2) exposures of seamount rocks in other Cape Verde islands (e.g., Brava; Maio, see Fig. 1); (3) previous geochemical and isotopic studies of rocks from Fogo and other Cape Verde islands.

Xenoliths found on Fogo consist of a suite of plutonic rocks ranging from dunites through pyroxenites to hornblendites. The least evolved varieties are composed of olivine and clinopyroxene in various proportions. ESM1 shows images of selected cumulate xenoliths, some

showing modal layering. More evolved lithologies include some that contain abundant apatite and haüyne. The xenoliths often show cumulus (poikilitic) textures and contain pools of alkali-rich glass that represent the final drops of melt from which the rocks crystallised. None of them are mantle peridotites (ESM 1), since their olivine Fo content and spinel Cr# do not plot within the "olivine-spinel mantle array" of Arai (1994), unlike the mantle xenoliths from the island of Sal (Bonadiman et al., 2005). Furthermore, they completely lack orthopyroxene, which is a characteristic component of mantle peridotites. Xenoliths derived from the lithospheric mantle and/or oceanic crust have not yet been found on Fogo, although such lithologies must be present in the lithosphere beneath the island. Mantle peridotite xenoliths are abundant in other Cape Verde islands (e.g., Ryabchikov et al., 1995; Shaw et al., 2006) and ocean-floor basalts have been found in Maio (Stillman et al., 1982). However, it appears that at least the shallower parts of the pathways through the lithosphere taken by the Fogo shield-stage magmas have been insulated from older lithospheric rocks by the various alkaline plutonic rocks that are found as xenoliths.

Some understanding of the range of pre-shield rocks present in the subsurface of Fogo can be obtained by a comparison with the islands of Brava and Maio (Fig. 1). Brava has experienced only limited subaerial volcanism and so has widespread exposures of uplifted seamount lithologies, including submarine volcanic rocks (hyaloclastites and pillow lavas) and plutonic intrusive rocks such as pyroxenites, ijolites, nepheline syenites and carbonatites (Madeira et al., 2010; Weidendorfer et al., 2016). In the much older and deeply eroded island of Maio, erosion has exposed seamount rocks formerly buried beneath the shield-stage volcanoes. MORB-type oceanic floor rocks are present on Maio, intruded by pyroxenites, essexites, syenites and carbonatites (Stillman et al., 1982). Xenoliths of MORB gabbros collected from seamounts to the SW of Brava (Barker et al., 2019) are also useful as samples of the local oceanic crust.

Previous collection and analysis of Fogo lava samples for bulk rock and isotope geochemical analysis has been undertaken by Gerlach et al. (1988), Davies et al. (1989), Doucelance et al. (2003), Escrig et al. (2005) and Cornu et al. (2021). The first three of these studies did not consider many samples, because they were intended for inter-island comparison, but the latter two focused on Fogo. There have also been several petrological and geochemical studies of samples from historical to recent Fogo eruptions (e.g., Hildner et al., 2011; Hildner et al., 2012; Mata et al., 2017; Klügel et al., 2020; Barker et al., 2023).

Determinations of pressures of last equilibration of Fogo magmas have been obtained using clinopyroxene-melt geobarometry and fluid inclusions (Hildner et al., 2011, 2012; Klügel et al., 2020; Lo Forte et al., 2023). These studies have identified a deep magma storage region at ca. 25 km below the island, within the oceanic lithospheric mantle, and several shallower reservoirs at pressures corresponding to 8–13 km depth, near the base of the oceanic crust but not necessarily within it. Pim et al. (2008) determined an oceanic crust thickness of about 9 km, including layers of sediments (1.7 km thick), a layer of probable oceanic crustal lavas 1.2 km thick, and an oceanic gabbro layer around 5 km thick. Their model shows a dense (2940 kgm^{-3}), high P-wave velocity (7000 ms^{-1}) crustal layer some 4–6 km thick, which we infer to be composed of olivine-rich refractory plutonic rocks. This layer could be the source of the ultramafic cumulate xenoliths on Fogo (ESM 1). In lavas from the 1995 and 2014–15 eruptions, studies showed a difference in pressure of clinopyroxene crystallization between the basanite/tephrite magma (higher pressures) and the phonolite magma (lower pressures) (Hildner et al., 2011; Klügel et al., 2020). This is interpreted as indicating the existence of a trans-crustal magma reservoir system in which the more evolved magmas are stored in the upper parts. Individual reservoirs may or may not have been internally stratified. Such stacked reservoirs provide the conditions for contamination of the alkaline magmas by lithologies in the crust and lithospheric mantle, although locations in the latter are suggested by the lack of identifiable oceanic crust xenoliths. A comprehensive study of fluid inclusions from pre- and post-collapse lavas on Fogo (Lo Forte et al., 2023) supports these general conclusions.

Previous investigations of the radiogenic isotope (Sr-Nd-Pb) compositions of rocks from Fogo are of great value in defining potential source end-members for the isotopic variations. As described by Escrig et al. (2005), when plotted on a diagram of $^{87}Sr/^{86}Sr$ vs $^{143}Nd/^{144}Nd$, all Fogo lava samples fall on a trend between the most depleted sample and at least one isotopically-enriched component. At least one component was considered to reside in the lithosphere. In a Sr-Nd-Pb isotope study of basalts from Sao Nicolau in the northern group of Cape Verde islands (Fig. 1), Millet et al. (2008) concluded that the isotopic variation was the result of interaction of the Cape Verde plume with several shallow-level components. In their model, the deep plume component had a radiogenic isotopic composition and had interacted with several lithospheric end-members, including Atlantic MORB, ocean crust and Cape Verde carbonatites.

2. Sample collection

In this study, lavas have been systematically sampled from the stratigraphically defined pre- and post-collapse Formations (Table 1), including (from oldest to youngest) the Bordeira Formation (24 samples), Ribeira Aguadinha Formation (10 samples), Monte Duarte Formation (29 samples), Portela Formation (21 samples) and Monte Orlando Formation (11 samples). In addition, in March 2015, 20 samples were collected from the 2014–15 eruption, from all distinct phases of the eruption, which form part of the Monte Orlando Formation. These samples were the same as those studied by Klügel et al. (2020). About 500–1000 g of sample were collected in most locations. We attempted to sample low vesicularity parts of lava flows, ideally from flow cores exposed in water-scoured channels or road-side outcrops. Sampling of pre-collapse lavas was undertaken in the collapse scar (Bordeira cliff), coastal cliffs, and in the walls of deep ribeiras where older pre-collapse lavas were exposed. Only two samples were taken from the lower parts of the Bordeira cliff, because much of this part of the Bordeira Formation has suffered from visible hydrothermal alteration. The rocks here are paler than those higher in the cliff when viewed from a distance, and greenish when viewed at outcrop.

Sampling of younger pre-collapse and most post-collapse and recent lava flows was easier, as they cover much of the island outside the collapse scar as well as infilling the collapse scar. They are accessible in the incised walls of dry river channels, in road cuts and other excavations, or as scoured flow tops in interfluve areas. Samples from coastal cliffs were only collected where there was no alternative, because of concerns about alteration and seawater spray contamination. Locations of all analysed samples are given in ESM Table 2 and those analysed for isotopes are shown in a Google Earth image in Fig. 3. Importantly, there is broad overlap between the regions in which the pre-collapse samples were collected and those in which post-collapse samples were collected, except for those from the Monte Orlando Formation which were erupted from vents within the Monte Amarelo collapse scar.

3. Analytical methods

Only samples that appeared fresh in both hand-specimen and thin-section were used for bulk-rock analysis (with two exceptions, discussed below, that were analysed to investigate the effects of hydrothermal alteration). Rock samples ~1 cm^3 were crushed with a stainless-steel jaw crusher that was cleaned with acetone between samples. The bulk rock powders were prepared using a tungsten carbide disc mill (ring and puck type). They were analysed using the X-ray fluorescence on the Panalytical Axios XRF instrument at Royal Holloway University of London. International standards used to calibrate the XRF included GA, GH, BR, GSN, DRN, FKN, DTN, ANG, BEN, MAN, ALI, IFG, BCR1, GSP2, BIR1, DTS1, DTS2, PCC1, BHVO1, AGV2, NIMG, NIMN, NIML, NIMS, NIMD and NIMP. Analysis of BCR-2, treated as an unknown, by the same method showed good agreement with recommended values

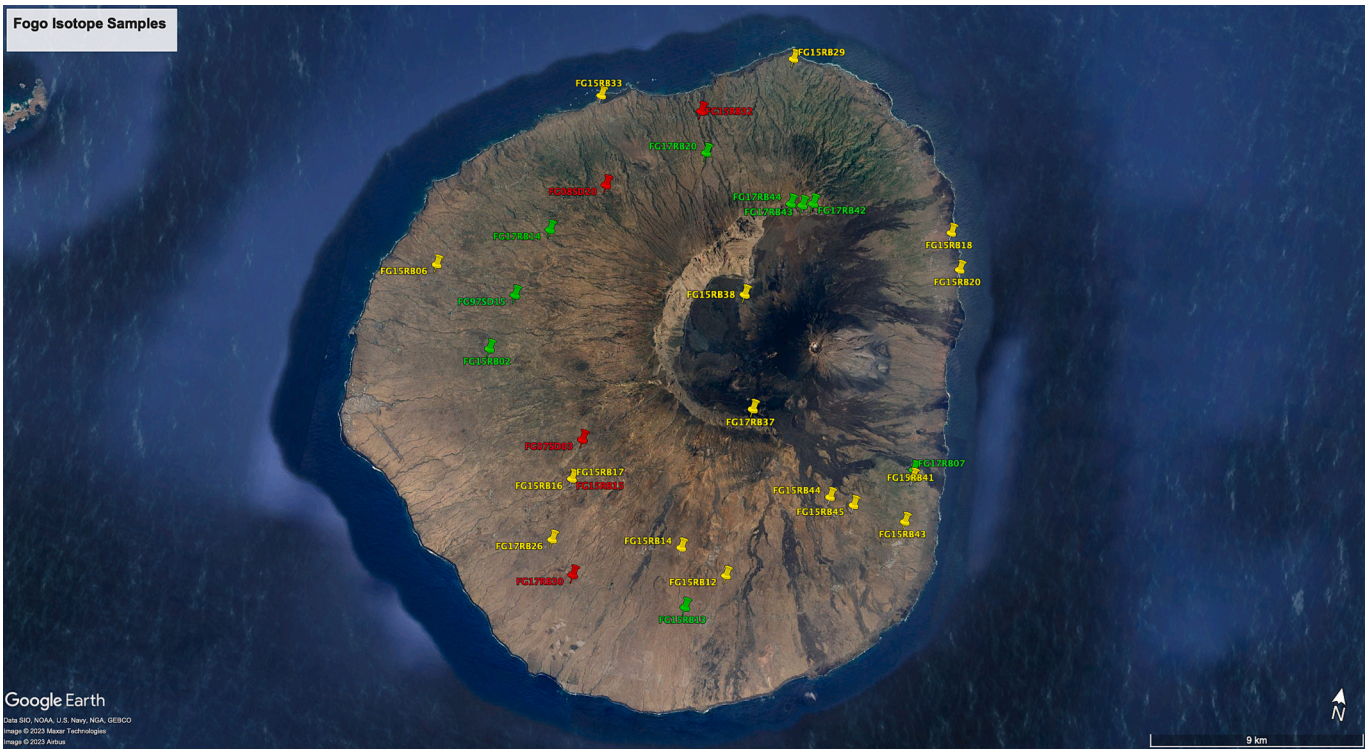

Fig. 3. Google Earth image of Fogo Island, with locations of pre-collapse (green pins), post-collapse (yellow pins) lava samples analysed for radiogenic isotopes, and high-P_2O_5 lavas (red pins). (For interpretation of the references to colour in this figure legend, the reader is referred to the web version of this article.)

(below 1% error for major element oxides, and up to 10% error for trace elements). Major elements were determined on fused glass discs, on a volatile-free basis with total Fe reported as Fe_2O_3. Loss on Ignition values were determined separately by igniting a weighed amount of powder (about 1 g) in an oven at 120 °C for 20 min and re-weighing (ESM Table 3). Trace elements were determined on pressed powder pellets. Results are given in the Supplementary Materials (ESM Table 3).

Solution ICP-MS analysis of trace elements was undertaken on 6 samples covering the range of MgO, to obtain the full spectrum of the Rare Earth Elements (REE) (ESM Table 4) using an Agilent 8800 ICP-QQQ-MS inductively coupled plasma mass spectrometer at the Open University, Milton Keynes, UK. Approximately 0.1 g of sample was weighed into clean Savillex containers. A mixture of 0.5 ml 15 M HNO_3 and 2 ml concentrated HF was added to the containers and sealed. These were boiled at 120 °C for 24 h and placed in a sonic bath for 20 min twice to ensure full dissolution. The solutions were then evaporated to near dryness before being dissolved in 2 ml of concentrated HCl and boiled at 120 °C overnight. They were again evaporated to near dryness before being dissolved in a mixture of 2 ml 15 M HNO_3 and 2 ml Milli-Q grade water and boiled at 120 °C for 4 h. The solutions were then added to Milli-Q grade water and made up to a volume to ensure 1000-fold dilution of the dissolved sample. One sample (FG15RB34) was analysed 5 times, as an internal monitor. An additional digest of the USGS reference standard BHVO-2 was prepared to assess accuracy and precision. A procedural blank was also processed and analysed with the samples.

At the start of the ICP-MS analytical runs, monitoring solutions, including 2% HNO_3 solution, Zr solutions at concentrations of 25 ppb, 50 ppb, 100 ppb and 150 ppb, were analysed, along with the BHVO-2 monitor. Between each *c.* 5 samples analysed during an analytical run, the reference monitor and a 2% HNO_3 solution monitor were analysed. The repeat measurements of BHVO-2 were used to assess precision and accuracy. Results for BHVO-2 and the internal standard are given in ESM 4.

Sr, Nd and Pb isotopes on 30 samples (plus 3 repeats) were obtained at the NERC Environmental Isotope Laboratory. Before dissolution, the crushates of these samples were washed in double distilled water using an ultrasonic bath, and then leached in 6 M HCl at about 80 °C, for 1–2 h. The samples were then centrifuged, the leachate discarded, the residues shaken up with milliQ H_2O, centrifuged again and the water discarded. This treatment was intended to remove any African dust and/or sea-water spray from the samples, since both of these surface contaminants may affect the radiogenic isotopic analysis, with the African dust being dominated by ancient crustal Sr, Nd and Pb isotopic components (Kumar et al., 2018), and the sea-water being dominated by radiogenic Sr (Farrell et al., 1995). After this leaching stage, the samples dissolved in a mixture of HF and HNO3. They were evaporated and converted to nitrate or chloride form. Sr and Pb were separated using SR-SPEC ion exchange resin following the methods of Deniel and Pin (2001). Nd was separated using a primary cation exchange column (Eichrom AG-50), followed by a LN-SPEC column. Samples for Pb isotopes were converted to bromide using 2 mls of concentrated HBr and Pb was separated using columns containing 100 ml of Dowex AG1x8 anion exchange resin. Procedural blanks for Sr, Nd and Pb were < 100 pg.

Sr fractions were loaded onto outgassed single Re filaments using a TaO activator solution, and analysed in multi-dynamic mode on a Thermo Scientific Triton mass spectrometer. Data were normalised to $^{86}Sr/^{88}Sr = 0.1194$. Measurements of the SRM987 Sr standard run gave a value of $^{87}Sr/^{86}Sr$ of 0.710254 ± 6 (1 sigma). Nd fractions were loaded onto one side of an outgassed double Re filament assembly using dilute HCl, and analysed in multi-dynamic mode on the same instrument. Data were normalised to $^{146}Nd/^{144}Nd = 0.7219$. Analyses of the JND-I standard gave a value of 0.512098 ± 11. All data are quoted relative to a value of 0.512115 for this standard. Prior to Pb isotope analysis, each sample was spiked with a Tl solution, to allow for correction of instrument-induced mass bias. Samples were introduced into the NU plasma MC-ICP-MS, using an ESI 50 μl/min PFA micro-concentric nebuliser. The accuracy and precision of the method was assessed by repeated analysis of a Tl-doped NBS 981 Pb reference standard and comparison with the known values of this reference material (Thirlwall,

2002). Results and uncertainties for all three isotope systems are given in ESM Table 5.

4. Results

4.1. Thin section petrography

Most of the Fogo lava samples are mafic rocks which are moderately to extremely porphyritic, with olivine and clinopyroxene being the main phenocrysts, together with Ti-magnetite. Olivine sometimes contains inclusions of Cr-spinel. A few lavas, distributed through the stratigraphy, are olivine-dominated "oceanites" with only sporadic and small clinopyroxene crystals (e.g., the undated Monte Preto de Sao Jorge eruption on the NW side of the island). A few lavas are more evolved tephrites and phonolites which can contain haüyne phenocrysts. Sparse amphibole, apatite, titanite and biotite phenocrysts are also found in these more evolved lavas. Plagioclase is very rare, being present as a groundmass phase in a few lavas (e.g., FG17RB43) and as microphenocrysts in sample FG17RB31. One fully-crystalline intrusive sample (not analysed by XRF) contains nepheline and leucite in its groundmass.

The petrographic features of two groups of lavas are slightly different from the others. Almost all rocks in the late pre-collapse Ribeira Aguadinha Formation are conspicuously porphyritic and dominated by clinopyroxene phenocrysts (up to 45% crystals), i.e., they are petrographically ankaramitic. In contrast, some evolved rocks from the older parts of the post-collapse Monte Duarte Formation are unusual for Fogo in being aphyric, whilst others have prominent haüyne and amphibole phenocrysts.

4.2. Major element geochemistry

Most of the post-collapse samples yielded negative LOIs (ESM Table 3), i.e., a gain on ignition due to oxidation of Fe^{2+}, whereas most of the pre-collapse samples had positive values. This indicates the post-collapse lavas are distinctly fresher than the pre-collapse ones, which have been subjected to a longer period of weathering and also hydrothermal alteration. Two samples from the lowermost part of the pre-collapse Bordeira Formation that has been visibly affected by hydrothermal activity (FG97SD17; FG97SD18) have high (2.2–2.4 wt%) LOIs (ESM Table 3) and are plotted as a separate group in the geochemical diagrams as "High LOI samples". A single Monte Duarte Formation sample with LOI of 1.6 wt% (FG17RB24) is a highly evolved phonolite with only 1.08 wt% MgO. This rock contains exceptionally high amounts of S (>2000 ppm) and halogens (1780 ppm Cl and 800 ppm F) that account for the high LOI.

The total alkali vs silica diagram (Fig. 4), divided into the five pre- and post-collapse Formations (Table 1), was used to classify the samples. They are mostly strongly silica-undersaturated basanites, tephrites and foidites (melanephelinites), although the post-collapse lavas also include two more evolved samples which trend towards phonolites. Samples from the 2014–15 eruption fall on the same trend as those of the other Monte Orlando Formation rocks which immediately pre-date them, but include some more evolved compositions otherwise only seen in samples from the earliest phase of the 1995 eruption (see below). The two high-LOI samples are very similar to the other Bordeira Formation samples on this plot, although they may have slightly high SiO_2 contents (Fig. 4).

Fig. 5 shows bivariate plots of major oxides against wt% MgO as an index of fractionation, with the samples again grouped into the five pre-collapse and post-collapse Formations. The major element compositions of the two "High-LOI" samples from the base of the Bordeira Formation, which are the oldest samples analysed in this study, are indistinguishable from all other Bordeira Formation samples.

The total range in MgO in Fogo lavas found in this study is 15.5–1.1 wt% (Fig. 5). Both pre- and post-collapse samples lie on similar trends, but the pre-collapse samples have a much narrower range of wt% MgO values than the post-collapse samples which show a much more complete trend across the entire range of MgO (Fig. 5). There is a lack of pre-collapse samples with MgO between 9 and 15 wt%, although a single strongly clinopyroxene-phyric rock from the Ribeira Aguadinha Formation (FG15RB13) has very high MgO (15.5 wt%). Also, the pre-collapse samples lack any rocks with <2 wt% MgO. However, both these observations may be due to a compositional dependence in our sampling bias against more visibly altered rocks, which may perhaps result from greater susceptibilities of high-MgO rocks and glassy phonolitic rocks to post-emplacement alteration.

Escrig et al. (2005) presented 17 bulk rock analyses from Fogo, with a total range in 10.8–4.6 wt% MgO, much narrower than the range in this study. Data from Munhá et al. (2006) also show a more limited range (9.0–1.5 wt% MgO). Barker et al. (2023) analysed 58 lava samples from historic eruptions, which show a wider compositional variation (1.8–11.8 wt% MgO). Our range of 1.1–15.5 wt% MgO is therefore more representative of the full range of lava flow compositions on the island, and more closely resembles that of Cornu et al. (2021) who showed a range of 13.26–1.61 wt% MgO. In ESM 6, we show a graphical comparison between our major element data for samples from the Monte Orlando Formation, including the 2014–15 eruption, and data from other studies of the same Formation. It shows that samples from the 2014–2015 eruption analysed in this study have extremely similar bulk rock compositions to those given by Mata et al. (2017). However, we were unable to collect a group of phonotephrites from the 1995 eruption, analysed by Hildner et al. (2011), because these outcrops were

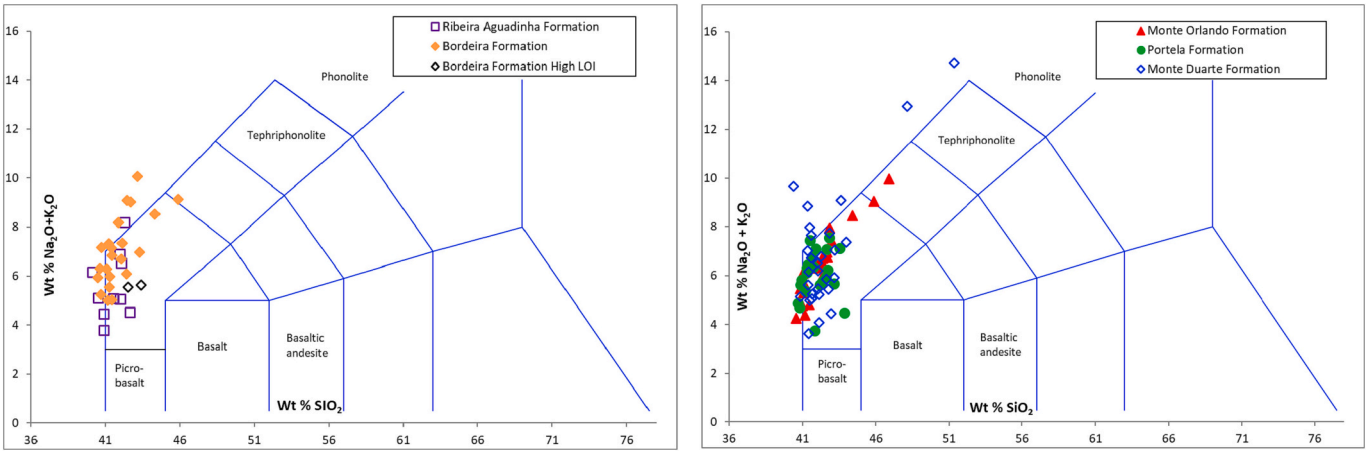

Fig. 4. TAS diagrams for pre-collapse and post-collapse lavas from Fogo including those of the 2014–15 eruption. Pre-collapse samples from the Bordeira cliff with high-LOIs are identified as black diamonds. Data from ESM Table 3.

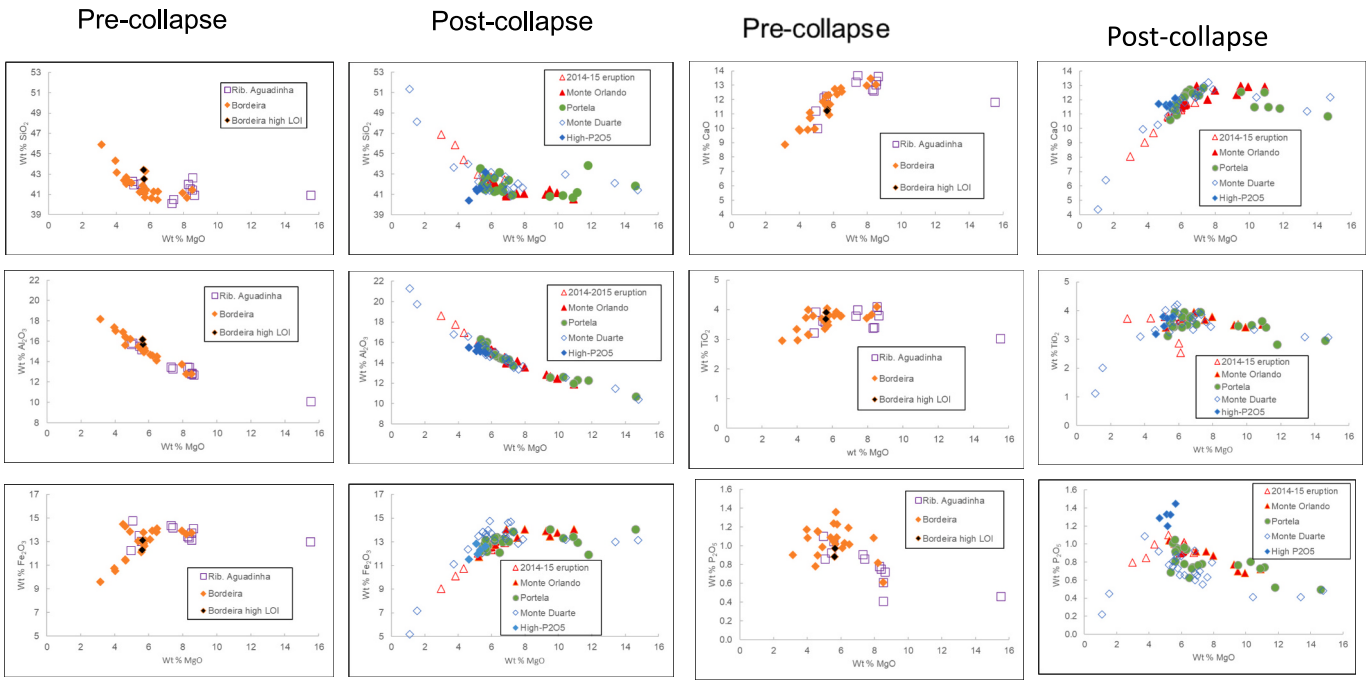

Fig. 5. Major element variation diagrams of bulk rock compositions of Fogo samples, divided into formation-level stratigraphic units, plus samples from the 2014–15 eruption analysed under the same conditions. "High-LOI" indicates two samples from the base of the Bordeira cliff which have been hydrothermally altered. Data from ESM Table 3.

inconveniently covered by the lavas of the 2014–15 eruption before we were able to collect samples.

Both pre- and post-collapse samples show a single overall evolutionary trend (Fig. 5), although the pre-collapse trend is less complete for the reasons discussed above. As MgO decreases, Al_2O_3 shows a continuous increase. In contrast, SiO_2 generally remains at 40–41 wt% until MgO reaches about 7 wt% and then increases to 51 wt% in the phonolites. A group of Ribeira Aguadinha Formation rocks with MgO ~ 8 wt% show a spread of SiO_2 contents from 41 wt% to 43 wt%, as well as other anomalous features discussed below. TiO_2 and CaO both show similar patterns in which they increase slightly over the interval of 16 to 8 wt% MgO, and then decrease to conspicuously low values as MgO reaches 1–2 wt%. Fe_2O_3 shows a similar pattern, but without the initial increase.

P_2O_5 values generally show an increase in the interval from 16 to 5 wt% MgO, and then some highly fractionated samples show a decrease (Fig. 5). However, the P_2O_5 vs MgO plot shows a distinct group of samples with conspicuously high P_2O_5 (>1.2 wt%). These samples (FG17RB30; FG15RB15; FG07SD03; FG08SD20; FG15RB32) are all from the early post-collapse eruptions of the Monte Duarte Formation. Their locations (Fig. 3) are all on the west or north-west side of the island, where they occur in flank eruptions. A few pre-collapse Bordeira Formation rocks also have similarly high P_2O_5 (for example, FG17RB28 with 1.36 wt% P_2O_5), but are less distinct from other Bordeira Formation rocks in the range 8 to 5 wt% MgO.

Several points of inflection can be identified in the bivariate diagrams shown in Fig. 5. The main one occurs between 7 and 8 wt% MgO, clearly seen in the trends of Fe_2O_3 and CaO. This is irrespective of the abundance of clinopyroxene phenocrysts as it is present in both the "ankaramitic" rocks of the Ribeira Aguadinha Formation and in other formations. Munhá et al. (2006) considered this inflection to be due to the onset of clinopyroxene fractionation, since this is the commonest high-CaO phenocryst, as plagioclase is largely absent. However, this inflection is more likely due to the cessation of olivine crystallization, which would have a similar effect. We consider this more likely because of the abundance of almost pure cumulate dunite xenoliths in some Fogo lavas (ESM 1), which probably represent the accumulated olivine crystals from this early fractionation stage. Ti-magnetite starts to fractionate at the same time, judging from the decrease of TiO_2 which starts at 7 wt % MgO, although this inflection is not as sharp as is seen from the onset of Ti-magnetite fractionation in other intraplate mafic volcanic suites (e.g., Tenerife; Neumann et al., 1999). The Al_2O_3 vs MgO trend for the Monte Orlando Formation and samples from the 2014–15 eruption also reveals a subtle change in slope at this point. In contrast, at about 5 wt% MgO, P_2O_5 begins to show a major decrease, implying apatite fractionation, although all the "high-P_2O_5" samples also have about 5 wt% MgO.

4.3. Trace elements

Fig. 6 presents a selection of trace elements plotted against wt% MgO. As in the major oxide plots (Fig. 5), all the Formations follow the same general trends, regardless of whether they are pre- or post-collapse. The two "High-LOI" samples are indistinguishable from the remainder of the Bordeira Formation samples except in having lower Rb, probably due to leaching by groundwater. Elements showing compatible behavior are Cr, Ni and (to some extent) Sc, as would be expected, whereas all others show some degree of incompatibility.

Mantle-normalised trace element diagrams for high-MgO lavas from Fogo, normalised to the data of McDonough and Sun (1995), are shown in Fig. 7. All samples show very similar patterns, with troughs at Pb and Th and low Y values. Only one high-MgO pre-collapse sample (FG15RB13) was available for analysis, but its pattern is identical to those of the post-collapse samples. Fig. 8 shows pyrolite-normalised incompatible trace element diagrams for the Monte Duarte Formation lavas, ranging from those with high MgO to the lowest MgO. Very little change is seen in the patterns, although the overall trace element contents tend to increase with fractionation. A comparison of the trace element diagrams of high- and low-P_2O_5 samples in Fig. 8 shows that the "high-P_2O_5" samples have higher contents of all incompatible trace elements except Pb.

Chondrite-normalised Rare Earth Element (REE) diagrams for six

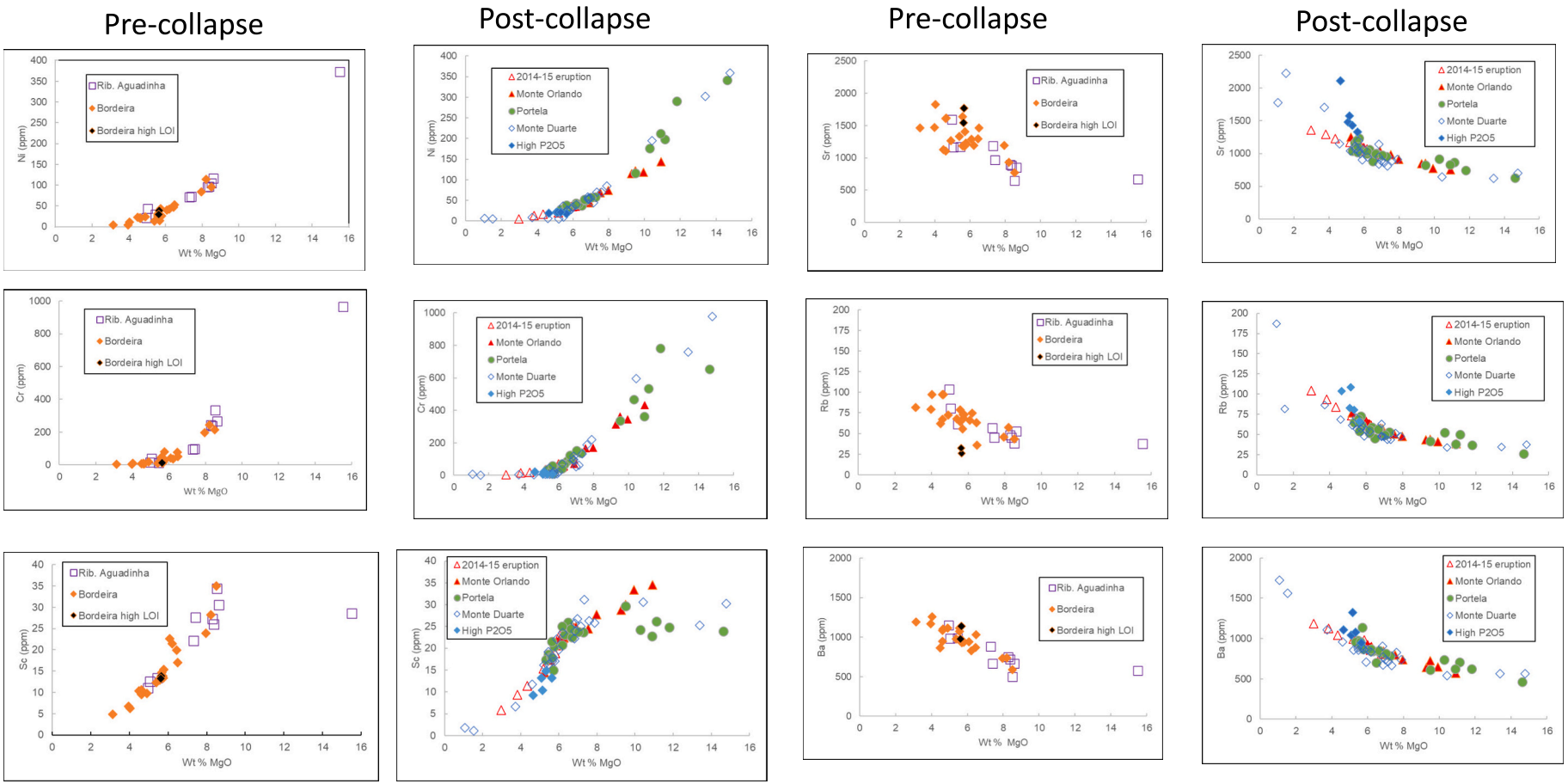

Fig. 6. Variation diagrams of selected trace elements vs MgO for pre- and post-collapse lavas from Fogo, including samples from the 2014–15 eruption. Data from ESM Table 3.

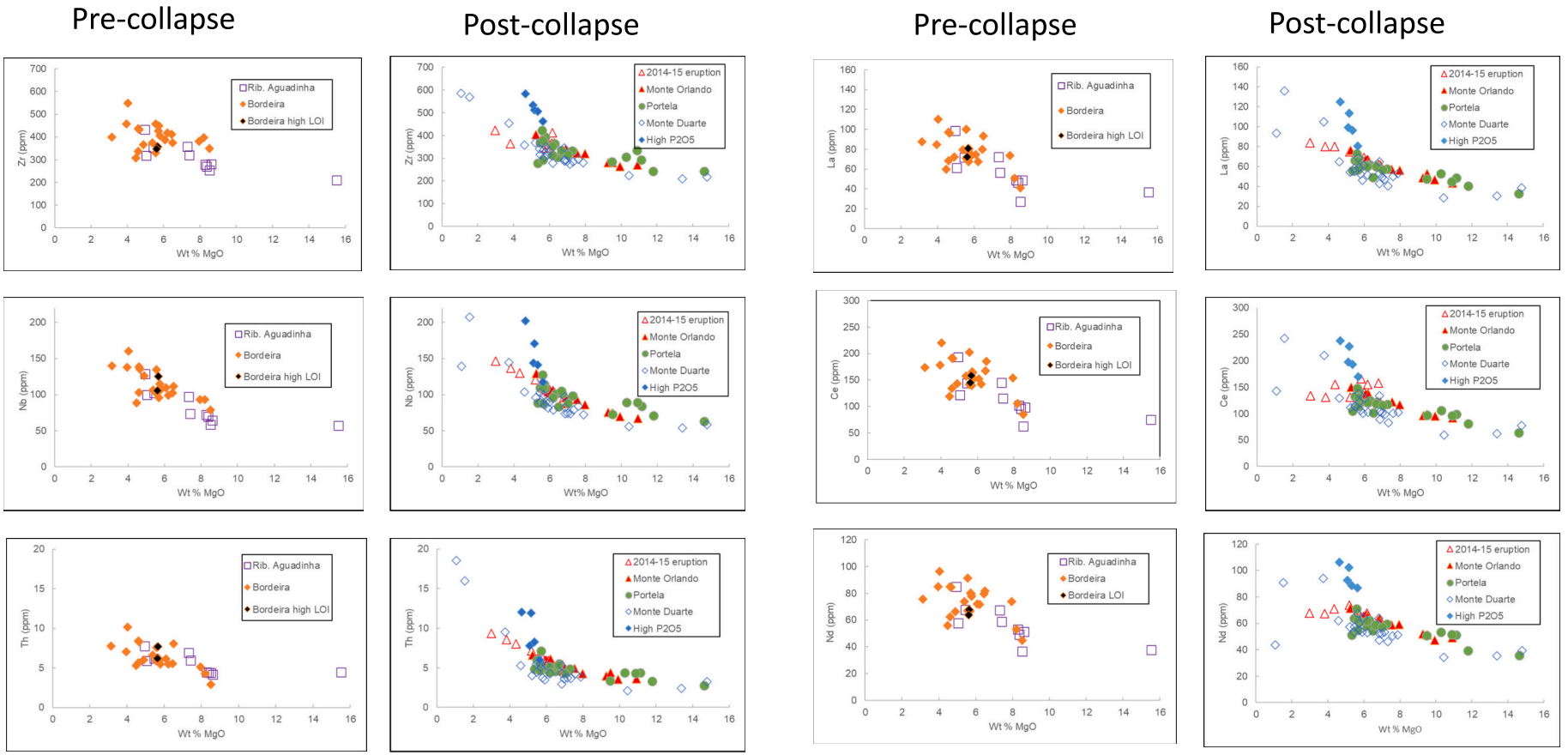

Fig. 6. (*continued*).

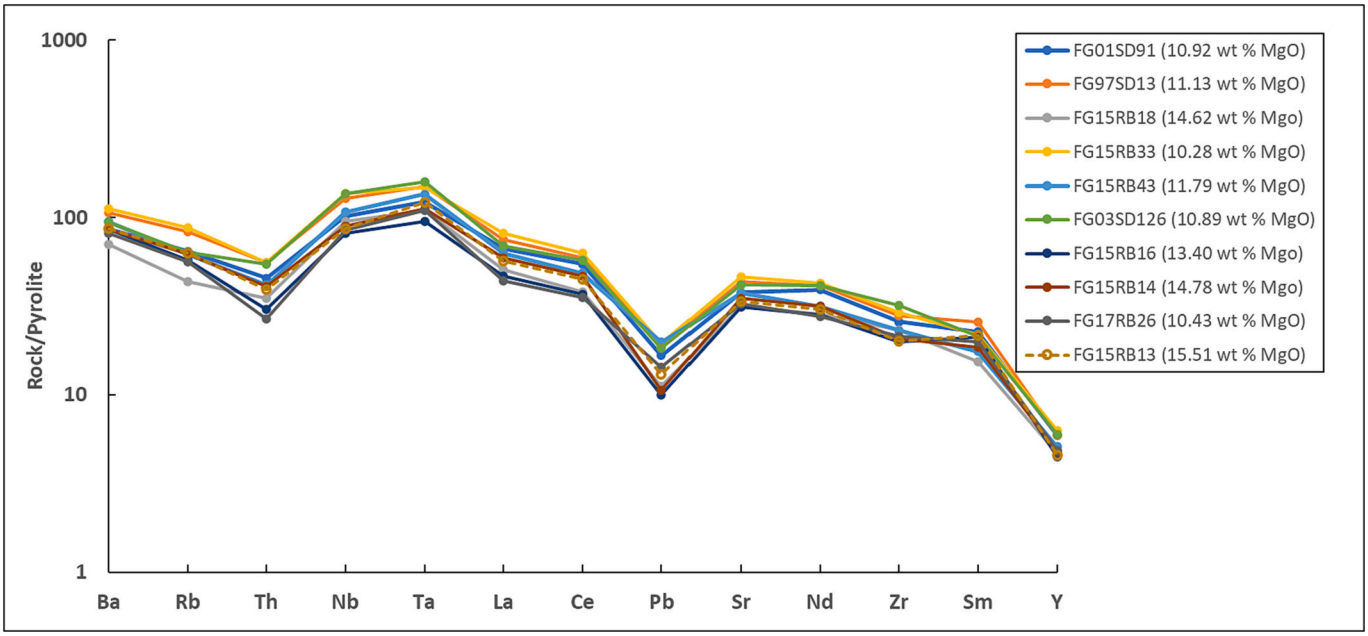

Fig. 7. Pyrolite-normalised trace element diagram for high-MgO lavas from Fogo (pre-collapse lava FG15RB13 shown in dashed line and open symbol). Data from ESM Table 3.

Fogo lavas covering a range of MgO (Fig. 9) show that, in general, all the REE increase with fractionation, except for the Middle Rare Earth Elements (MREE) in phonolite FG17RB24 which show a significant depletion. This is probably related to very late-stage fractionation of titanite, which has high distribution coefficients for the MREE (Melluso et al., 2018). The "high-P_2O_5" sample for which a full REE pattern is available (FG08SD20) has the highest REE contents, despite not being the most evolved lava (Fig. 6).

4.4. Sr-Nd-Pb isotopes

Samples for isotopic analysis were chosen to cover the range of stratigraphic Formations (Table 1) and to avoid where possible samples that could have been affected by wind-blown dust or seawater (Fig. 3).

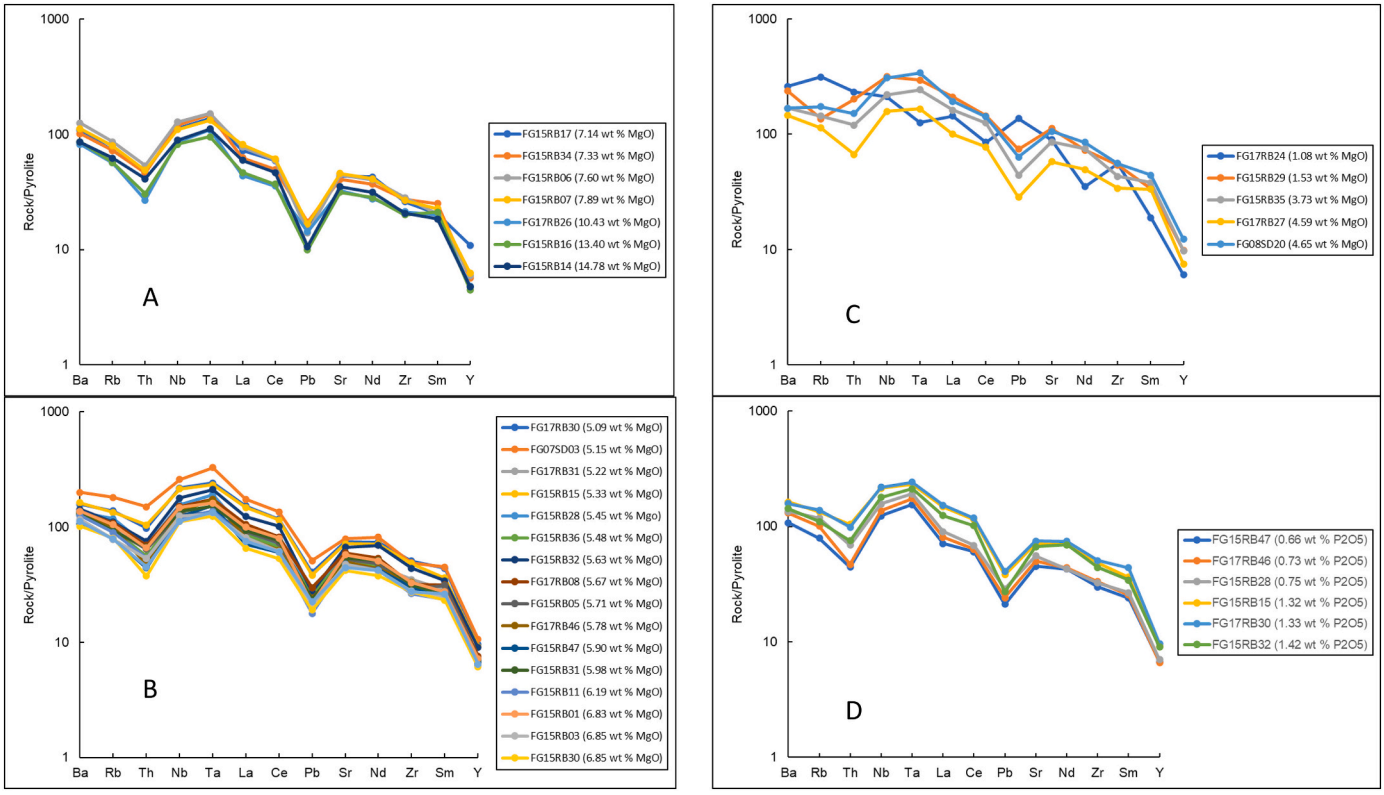

Fig. 8. Pyrolite-normalised trace element diagrams showing representative Monte Duarte samples. (A) = samples >7 wt% MgO; (B) = samples with 7–5 wt% MgO, (C) = samples 5–0 wt% MgO; (D) = samples with >1.24 wt% P_2O_5. Data from ESM Table 3.

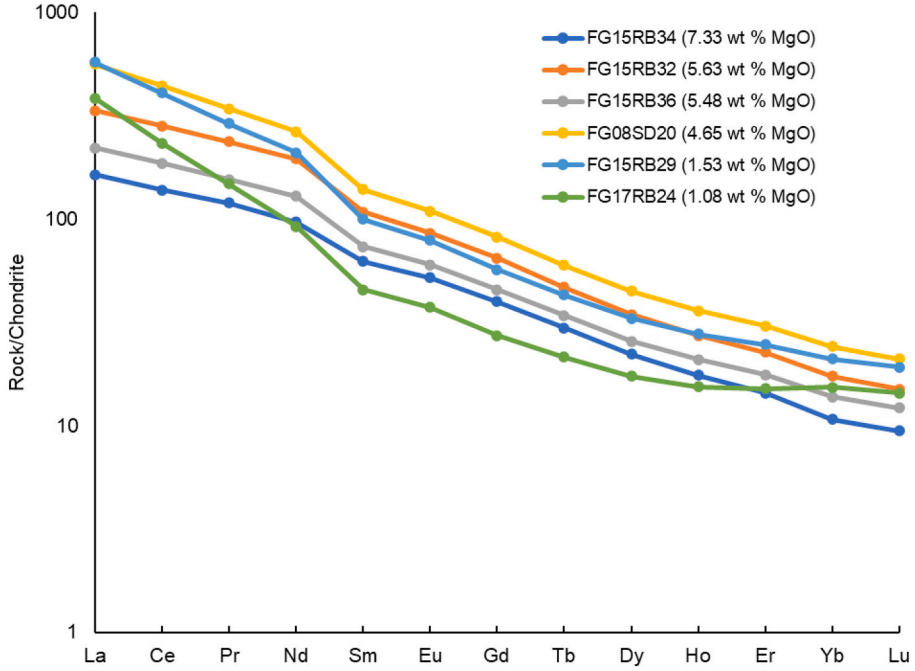

Fig. 9. Chondrite-normalised REE for post-collapse lavas from Fogo with varying MgO contents. Samples FG08SD20 and FG15RB32 are high-P_2O_5 type. Sample FG17RB24 is a phonolite. Data from ESM Table 4.

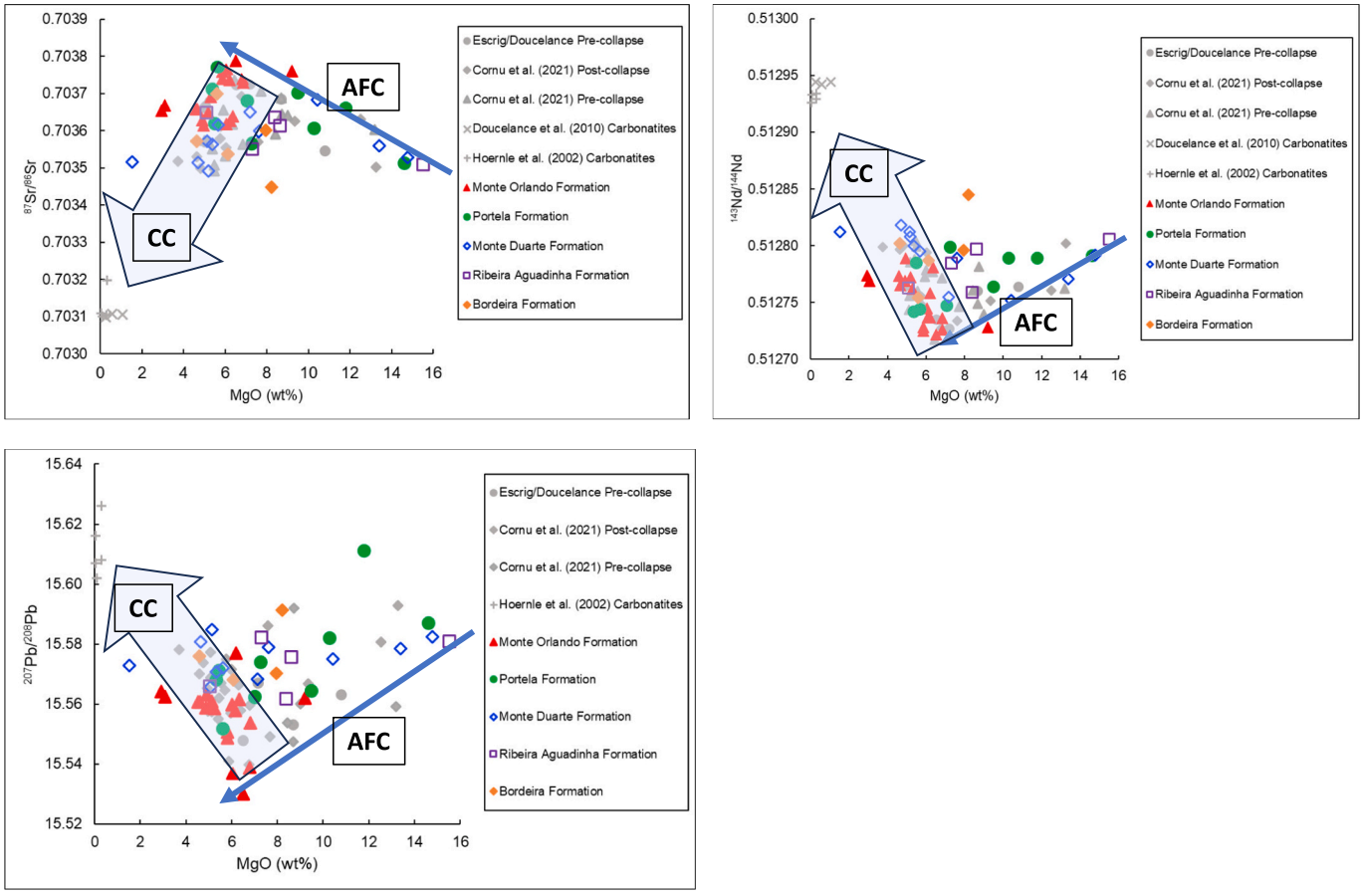

Fig. 10. Plot of wt% MgO vs $^{87}Sr/^{86}Sr$, $^{143}Nd/^{144}Nd$ and $^{206}Pb/^{204}Pb$ for samples from this and previous studies of Fogo. FC = trend of fractional crystallization; AFC = trend of assimilation and fractional crystallization; CC = trend towards carbonatite contamination. Data from ESM Table 5. Isotope data for the Monte Orlando formation are taken from the 2014–15 eruption (Mata et al., 2017) and the early historic eruptions (Escrig et al., 2005), but the Pb-isotope data of Escrig et al. (2005) have been excluded because they were not analysed using Tl-doping or double spiking techniques.

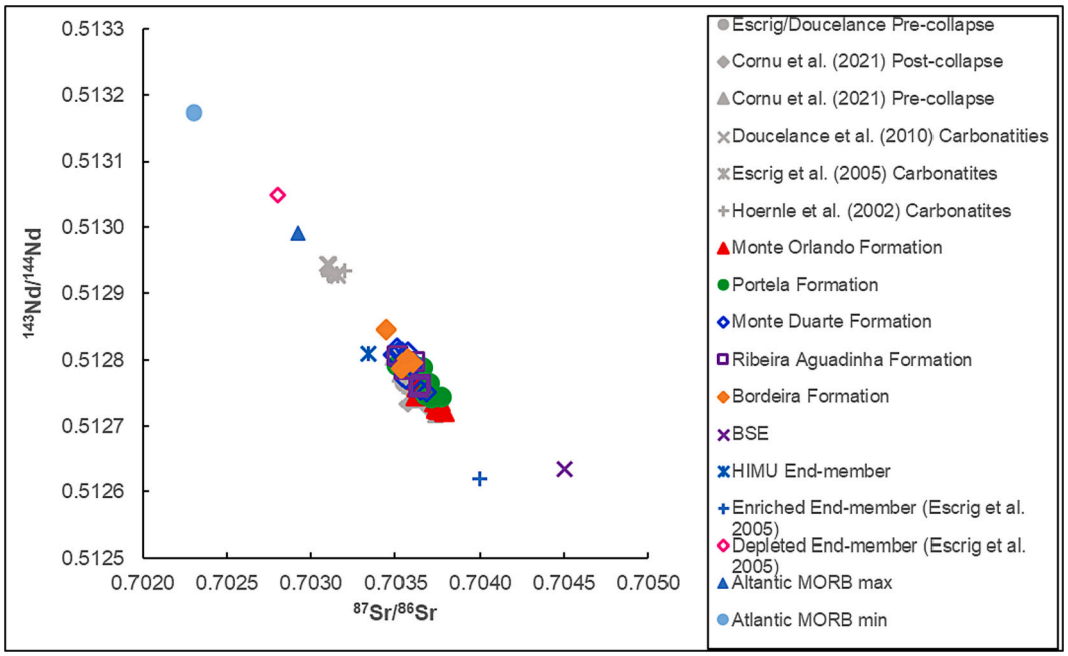

Fig. 11. Sr-Nd isotope compositions of lava samples from Fogo analysed in this study (Data from ESM Table 5) compared with previous studies. Isotope data for the Monte Orlando formation are from the 2014–15 eruption (Mata et al., 2017) and some historic eruptions (Escrig et al., 2005).

Five samples were analysed from the Bordeira Formation; 5 from the Ribeira Aguadinha Formation; 11 from Monte Duarte Formation and 9 from the Portela Formation. Data for the Monte Orlando Formation have been taken from the study of the 2014–15 eruption by Mata et al. (2017) and the dated historical eruptions (Escrig et al., 2005). The similarity between our results and those of previous studies is shown in Fig. 10, where wt% MgO is plotted against $^{87}Sr/^{86}Sr$, $^{143}Nd/^{144}Nd$ and $^{206}Pb/^{204}Pb$ for our samples and compared to previous data. Our samples show the same range and trends as those previously analysed.

The combined Sr and Nd results for our 30 samples are shown on Fig. 11 along with isotopic data points from other studies. They show a range in both $^{87}Sr/^{86}Sr$ (0.7034 to 0.70375) and $^{143}Nd/^{144}Nd$ (0.51273 to 0.51284), and a negative correlation. The results are in good agreement with those of previous studies, except for one (pre-collapse) Bordeira Formation sample (FG17RB44) which has a distinctly more depleted isotope signature (low $^{87}Sr/^{86}Sr$, high $^{143}Nd/^{144}Nd$) than any previously analysed Fogo lava. The three high-P_2O_5 samples from the Monte Duarte Formation show relatively high $^{143}Nd/^{144}Nd$ values, but overlap with results for samples from pre-collapse Formations. Our Pb isotope data also broadly agree with those of previous studies (Fig. 12) but show a tighter trend at a shallower angle to the NHRL than previous results. The most depleted sample in Sr-Nd isotope space also shows the highest $^{206}Pb/^{204}Pb$, lying on the NHRL. Plots of $^{87}Sr/^{86}Sr$ against Pb isotope compositions for samples from this study (ESM Table 5) form straight line trends (not shown).

Our data do not show any marked difference in isotope ratios between the pre- and post-collapse lavas when isotope compositions are plotted in stratigraphic order by Formation (Fig. 13). There is a similarly wide range of isotopic composition in all Formations irrespective of their durations, and fully overlapping ranges in the Formations immediately below and above the collapse. However, the isotope data show an overall increase in $^{87}Sr/^{86}Sr$ and a slight decrease in $^{143}Nd/^{144}Nd$ and $^{208}Pb/^{204}Pb$ over time (Fig. 13), i.e., an increase in the contribution of a more enriched source.

5. Discussion

5.1. Magma fractionation

Our analyses of nearly 100 Fogo shield-stage lavas show a common broad fractionation trend throughout the sub-aerial eruptive history of the island (Figs. 5,6). The most primitive lavas (8–15.5 wt% MgO) experienced fractionation of olivine and Cr-spinel, as shown by the inflection point at 8 wt% MgO. This was followed by fractionation of abundant clinopyroxene, shown by the change in slope of the CaO-MgO plot (Fig. 5) and the crystallization of more Fe-Ti-rich spinel. The most common erupted compositions are in the 8–6 wt% MgO bracket, when olivine ceased to crystallise and clinopyroxene became the most common phenocryst. Spinels formed throughout this range of magma compositions. They show a continuous progression from early Cr-spinels through to Ti-magnetite and so produce a gradual increase in the compatibility of Ti rather than a sharp inflection in the TiO_2 vs MgO plot (Fig. 5). The more evolved phonolitic magmas with 1.1–4 wt% MgO also crystallised apatite with titanite, accounting for the decrease in P_2O_5 (Fig. 5) and the MREE (Fig. 9). The plots shown in ESM 6 for the Monte Orlando Formation, which include data from other studies, demonstrate the same fractionation trends.

Fractionation of the observed phases (olivine+Cr-spinel; cpx + Fe-Ti oxides; apatite+biotite+titanite) is also reflected in the trace element diagrams (Fig. 6). Both Ni and Cr decrease with decreasing MgO content, suggesting simultaneous fractionation of olivine and Cr-spinel. In contrast, the plot for Sc, which is governed by clinopyroxene fractionation, closely follows those of Fe_2O_3 and CaO, with a flat trend at high MgO values, changing to a decreasing trend at 8 wt% MgO. Large Ion Lithophile Elements (LILE) such as Sr and Ba show incompatible behavior, demonstrating a lack of involvement of feldspar in the fractionation sequence. High field strength elements (HFSE) such as Zr, Nb and Th are mostly incompatible over the entire range of MgO contents. The "high-P_2O_5" lavas also show conspicuously high concentrations of the Light Rare Earth Elements (LREE), Sr, Zr and Nb. In Fig. 8, the most evolved lavas from the Monte Duarte Formation show a decrease in Rb and Nb-Ta, indicating fractionation of biotite and titanite, respectively.

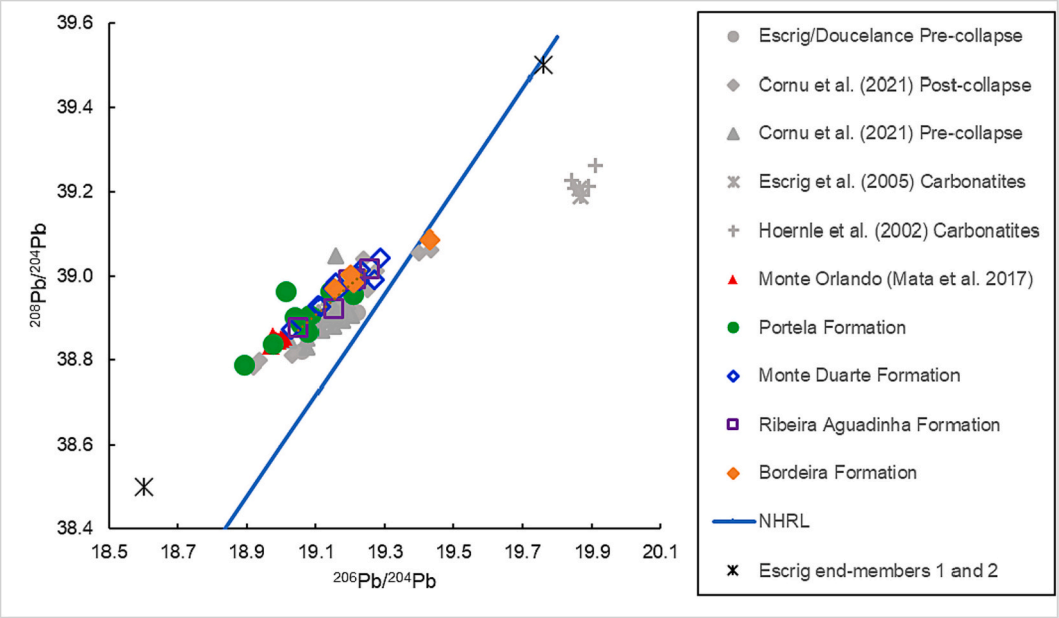

Fig. 12. Pb isotope compositions of Fogo samples from this study, compared with those of previous studies. Data from ESM Table 5. Blue line is NHRL. Isotope data for the 2014–15 eruption (Mata et al., 2017) represent the Monte Orlando formation. (For interpretation of the references to colour in this figure legend, the reader is referred to the web version of this article.)

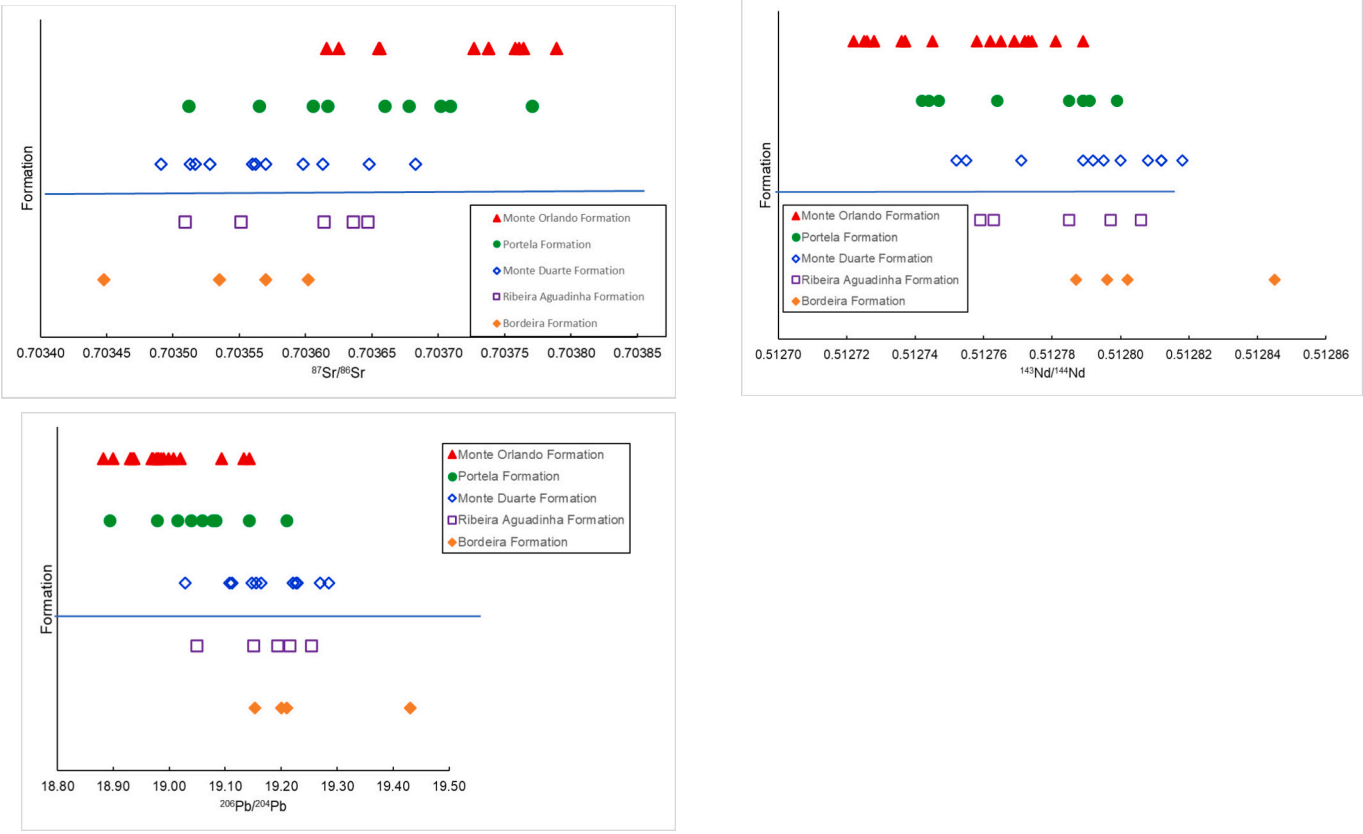

Fig. 13. Plots of Sr, Nd and Pb isotope data for Fogo lavas, in stratigraphic order by Formation. Data from ESM Table 5. Isotope data for the 2014–15 eruption (Mata et al., 2017) and some historic eruptions (Escrig et al., 2005) represent the Monte Orlando formation.

5.2. Apparent crystal accumulation

There is no indication that the high titanaugite content of the Ribeira Aguadinha rocks has had a significant effect on the CaO and TiO_2 contents (Fig. 5), compared to more phenocryst-poor rocks. Some of the "ankaramitic" rocks of the Ribeira Aguadinha Formation show elevated Sc (Fig. 6), and this is the only indication that any of these rocks may contain accumulative clinopyroxene. We suggest that an unusually high

partition coefficient for Sc into these pyroxenes from the extremely silica-deficient magma may be involved. Thus, almost all of the clinopyroxene phenocrysts are not actually accumulative but reflect late-stage crystallization during magma ascent such that there was insufficient time for compositionally-significant crystal settling. Similarly, data for the "oceanites", occasionally found in post-collapse Formations, do not show any unusual contents of compatible trace elements such as Cr and Ni (Fig. 6), indicating again that these lavas are not accumulative in nature. The greater scatter in the Cr data for high-MgO rocks, as compared to the Ni data, may simply reflect random variation in the number and size of chromite grains in each of the aliquots in the powdering stage of sample preparation.

5.3. Primitive magmas and mantle heterogeneity

The most primitive lavas in our sample suite are those with 13–15 wt % MgO (Figs. 5 and 6). These values are higher than previously found on Fogo, but not as high as those reported by Holm et al. (2006) for the island of Santo Antao in the northern Cape Verde islands which reach 19 wt% MgO. We therefore choose to define the isotopic characteristics of the deep plume component as being those shown by the highest MgO rocks (Fig. 10).

Previous isotopic studies have shown that plume magmas feeding Fogo's volcanoes are sourced from a combination of the HIMU and EM1 mantle reservoirs (Escrig et al., 2005). Jackson et al. (2018) provided strong evidence that both HIMU and EM reservoirs are normally situated in the deep mantle, but that Cape Verde is anomalous in showing the presence of both sources in its lavas. It is therefore most likely that one of these reservoirs is present in the lithosphere beneath Cape Verde. Our conclusions regarding the isotopic end-members represented in our Sr-Nd-Pb data differ from those of Escrig et al. (2005) in that there is no evidence in our samples for significant assimilation of oceanic crust, neither in the geochemical data or in the xenolith assemblages. However, the most isotopically depleted samples on the Sr-Nd isotope trend (Fig. 11) point towards the compositions of carbonatites from Fogo (Hoernle et al., 2002). Our study has also revealed a trend towards a more isotopically enriched component (or conversely, a decrease in an isotopically depleted component) with time (Fig. 13). This trend is not evident in the less extensive sampling of Fogo by Escrig et al. (2005) and is not seen in the Millet et al. (2008) study of Sao Nicolau lavas in the northern Cape Verde islands.

On Fig. 12, the trend of Pb isotopes points towards the compositions of Fogo carbonatites which have higher Pb-isotope compositions. All other samples plot in a trend away from the NHRL towards an enriched end-member which differs slightly from that defined by Escrig et al. (2005). The enriched component probably resides in the old sub-oceanic lithospheric mantle beneath Fogo, because crystallization depths of phenocrysts are between 40 and 20 km (Klügel et al., 2020). Also, the AFC trends seen in Fig. 10 imply interaction of magma with colder lithospheric material, with fractionation being driven by large temperature differences between the magma and the lithosphere.

Because all isotope plots for the data in this study form straight lines (Figs. 11, 12), modelling would be simple two component mixing between end-members with similar incompatible trace element ratios. The end-members for the AFC trend (Fig. 10) are a plume component (shown by the high-MgO lavas) and a more isotopically enriched lithospheric component, whereas the end-members for the carbonatite-contamination trend are the products of the AFC trend and the local carbonatites on Fogo.

5.4. Contamination

The "high P_2O_5" group of lavas in the Monte Duarte Formation that have unusually high incompatible trace element contents (Fig. 8) are all relatively evolved with 4.6–5.6 wt% MgO, but other Monte Duarte Formation rocks with similar MgO contents are markedly lower in P_2O_5 and incompatible trace elements (Fig. 6). The most likely explanation for this "high-P_2O_5" group is interaction of their magmas with older intrusive carbonatites in the seamount beneath Fogo. The enrichment in P_2O_5 cannot be due to interaction with evolved silicate rocks because such rocks will have crystallised from magmas that have experienced apatite fractionation (Fig. 5), and hence will have low P_2O_5. Barker et al. (2023) have also suggested that some historical eruptions on Fogo were contaminated by local carbonatites. Interaction with carbonatites could take the form of bulk assimilation or an AFC process, and may also account for the features of the few Bordeira Formation rocks which have similarly high-P_2O_5 and are also enriched in incompatible trace elements. The reduced contrast between these rocks and most other Bordeira Formation rocks reflects a broad tendency to higher incompatible element concentrations in the Bordeira Formation as a whole, as compared to rocks of the younger Ribeira Aguadinha and Monte Duarte Formations (Figs. 5, 6 and 8).

Conversely, the group of high-SiO_2, low-P_2O_5 rocks with ~8 wt% MgO in the Ribeira Aguadinha Formation also have low contents of Sr, Ba, Nb, La, Ce and Nd. Whilst these samples also have high Sc and possibly Cr, suggesting some accumulation of Sc-rich and perhaps Cr-rich clinopyroxene, the major elements do not support this. In particular, CaO contents are not elevated as they would be with only minor titanaugite accumulation. A possible explanation of this is that the magmas that formed these particular Ribeira Aguadinha Formation rocks, and perhaps also some post-collapse rocks with higher SiO_2 and lower P_2O_5 and incompatible elements, experienced relatively little interaction with Si-poor, trace element-enriched, apatite-bearing carbonatite, compared to almost all the other rocks sampled in this study.

Fig. 10 shows Sr-isotope data for Fogo lavas in this study, along with data by previous workers, plotted against wt% MgO as a fractionation index. They fall into a broad triangle, with its upper edge defined by an inclined trend towards higher $^{87}Sr/^{86}Sr$ compositions with decreasing MgO, interpreted as a trend of coupled assimilation-fractional crystallization (shown as "AFC" on Fig. 10). Below this limiting trend, across the whole range of MgO values but with a possible tendency to greater offset in more evolved rocks, there is a wide spread in $^{87}Sr/^{86}Sr$ values towards the values of Fogo carbonatites (Hoernle et al., 2002; Doucelance et al., 2010). This spread is represented by a broad arrow labeled "CC" in Fig. 10. The same triangular data distribution and AFC / CC trends can also be seen in plots of Nd and Pb isotopes vs MgO (Fig. 10). The spread of values on the "CC" trend is greatest in more evolved rocks with higher Sr, Nd and Pb concentrations that were erupted as lower temperature magmas than were the less evolved lavas with higher MgO contents. This implies that the "CC" trend is due to contamination that was decoupled from fractional crystallization and that took place after the production of the ranges of both chemical and isotopic compositions due to AFC. A two-stage magma contamination process, involving different mechanisms as well as different contaminants, is therefore implied. These trends of variation in isotopic composition with MgO values also confirm our inference that the high-MgO rocks are not simply derived from lower-MgO rocks by phenocryst accumulation, since if they were accumulative then they would show the same wide ranges of Sr, Nd and Pb isotopes.

The coupling of assimilation to magma evolution by cooling and fractional crystallization in the AFC trend suggests that the isotopically-enriched end-member assimilant was present deep in the mantle lithosphere where fractionation took place. This is below the depths of last crystal equilibration before eruption, which are 20 to 25 km as indicated in the phenocryst rim equilibration studies of Hildner et al. (2011, 2012) and Klügel et al. (2020). Hildner et al. (2012) have shown that Fogo is fed by a vertically stratified magma plumbing system, with primitive magmas mainly fractionating at greater depths than the more evolved magmas. Our data suggest that AFC occurs in the primitive magmas at greater depths, whereas carbonatite contamination occurs at shallower depths in all but the least-evolved magmas.

5.5. Effects of sector collapse and pre-collapse instability

This study of pre- and post-collapse lavas from Fogo shows that there is no obvious difference between the two groups (Figs. 5, 6), except perhaps that the range of compositions of the post-collapse Monte Duarte Formation is slightly greater than that seen in pre-collapse rocks. However, this represents most of the post-collapse period, so it is longer than that of any other Formation and a larger number of samples were collected from this Formation than any other. Although there is no evidence for an abrupt shift in major and trace element concentrations between pre- and post-collapse rocks, some broad trends can be seen with time from the base of the sampled Bordeira Formation to the most recently-erupted historic lavas of the Monte Orlando Formation. These include: (i) a lower abundance of high-MgO rocks in our pre-collapse samples, that can be attributed to a combination of generally increasing alteration of such rocks with age and our sampling bias against visibly altered rocks; (ii) a broad trend through time towards lower concentrations of incompatible elements, especially those liable to be enriched in apatite-bearing carbonatite rocks; (iii) wide compositional scatter associated in part with groups of lavas with distinctive characteristics, such as the "high-P_2O_5" lavas in the Monte Duarte Formation and their counterparts in the Bordeira Formation.

The only clear change identified as occurring in the pre-collapse period, the switch to eruption of the highly porphyritic "ankaramitic" magmas that characterize the Ribeira Aguadinha Formation, is not associated with corresponding changes in major element, trace element and isotopic compositions. The abundant titanaugite phenocrysts in the Ribeira Aguadinha formation rocks were not accumulative for the most part, since they show no effect upon bulk rock composition other than a small increase in Sc and possibly Cr. Instead they have largely formed just before magma ascent and eruption, in a period of crystallization that was short compared to timescales of crystal separation and consequent magma fractionation. Further studies of compositional zonation and diffusional reequilibration in these phenocrysts are needed to quantify these timescales and the mechanisms and processes of crystallization. However, this crystal growth would have increased magma density and therefore tended to reduce the density difference between magma and wall rocks that is a key driver of magma ascent. One compensating density-decreasing process might have been volatile exsolution and bubble formation associated with phenocryst crystallization. However, the eruption of these highly porphyritic magmas during the structural reorganization of the Monte Amarelo volcano prior to its sector collapse (Fig. 2) suggests that factors such as the onset of incipient flank instability and a reduction in magma overpressures may have also been involved.

In contrast to the present study, Cornu et al. (2021) found a change in bulk rock composition across the Monte Amarelo collapse. In their study, in which they collected lavas mainly from the Bordeira cliff, Cornu et al. (2021) identified a suite of lavas enriched in incompatible elements (Na, K, La, Pb, Th) which appears to have been erupted immediately after the collapse. These are not the same as our "high-P_2O_5" rocks because the samples they identified as being enriched in REE do not have anomalously high P_2O_5 contents. It is likely that the apparent discrepancy between the compositional trends identified in this study and the conclusion of Cornu et al. (2021) that a distinct compositional shift occurred at the time of the collapse, may simply be due incomplete sampling of the full range of rock compositions on Fogo. It seems that even the large numbers of samples collected and analysed both for this study and that of Cornu et al. (2021) are insufficient to represent the full range of lava compositions on the island, owing to exceptionally wide compositional variability in erupted magmas. In such a situation, apparent differences in compositional trends may result from different sampling strategies and/or differences in the spatial distributions of samples collected for different studies.

Isotope compositions of our analysed lavas also show no greater differences between the immediately pre- and immediately post-collapse samples than is seen both within and between the five Formations (Fig. 13). Our data, combined with those of Mata et al. (2017) and Escrig et al. (2005), indicate an overall temporal trend towards a more enriched component with higher $^{87}Sr/^{86}Sr$, or a decrease in a more depleted component. However, within each Formation, largely irrespective of its duration, there is a similarly large spread in all isotopic compositions. This points to the presence of large, short-term variations in the isotopic compositions of erupted magmas, between and even within eruptions. This can be clearly seen in the 2014–15 eruption products which show a wide range of Sr and Nd isotopes, as much as half of that seen in our sample sets from entire Formations (Fig. 13). Whereas the isotope data from the 2014–15 eruption were interpreted by Mata et al. (2017) as being evidence for small-scale mantle heterogeneity, we consider that they indicate different amounts of shallow contamination at a late stage in magma evolution (Fig. 10).

The combination of these two patterns of isotopic variation, short-term and very long-term, suggests that successive erupted magma batches take different pathways, assimilating different amounts of different contaminants, through an isotopically heterogeneous lithosphere containing a fusible contaminant that has become significantly less abundant over time. Specifically, we consider that the long-term isotopic trend towards more isotopically enriched compositions (Figs. 11 and 12) is due to extraction and exhaustion of fusible, incompatible element-enriched but isotopically depleted carbonatite from this volume of lithosphere.

Our isotope results are unlike those of Cornu et al. (2021), who argued for a step change in isotope characteristics at the time of the Monte Amarelo collapse. Our approach of using the five defined stratigraphic Formations as data bins (Table 1, Fig. 13) allows us to compare this proposed step change with the isotopic variations that occur within both long-duration and short-duration stratigraphic Formations, and even within single well-sampled eruptions such as 2014–15 (Mata et al., 2017). Fig. 13 shows no evidence of any distinct isotopic excursion or shift at or around the time of collapse that matches, let alone exceeds, these short-term variations that exist within all of our Formations. Therefore, as with the major and trace element variations, apparent differences in isotopic trends identified in different studies, for volcanoes with as much compositional variation as is present on Fogo, may simply result from different sampling strategies. Our sampling strategy covered the entire island (Fig. 3), whereas Cornu et al. (2021) concentrated on sampling vertical sections of the Bordeira cliff. Thus, some of the differences between our interpretation of the geochemistry of Fogo lavas and that of Cornu et al. (2021) may lie in the different sampling and dating strategies.

6. Conclusions

This study of the shield-stage lavas erupted before and after the Monte Amarelo collapse on Fogo (Cape Verde islands) has divided the stratigraphy into five Formations. Two are older than the collapse (Bordeira, Ribeira Aguadinha), whereas three are post-collapse (Monte Duarte, Portela and Monte Orlando). The lavas cover a wide range of major element compositions from melanephelinites to phonolites, resulting mainly from fractional crystallization of the observed phenocryst phases. Radiogenic isotopic data suggest a plume source for the high-MgO lavas, together with two contaminants that have affected the more evolved magmas, one of which may reside in the mantle lithosphere and the other may be the local plutonic carbonatites. The five Formations show very similar ranges of variation in radiogenic isotopes, regardless of the length of time covered by each Formation.

The study was undertaken without any preconception regarding whether there would be a chemical or isotopic change in the magmas related to the Monte Amarelo collapse. It shows no unusual abrupt shift in major, trace element or isotope compositions between lavas erupted before and after the collapse, but has identified an overall secular change towards more enriched isotopic compositions, and less enriched

trace element contents, in more recently erupted lavas. Eruption of highly porphyritic "ankaramitic" magmas just prior to sector collapse may be related to the onset of instability in the volcanic edifice.

Author statement

BRB collected, prepared and analysed all the samples, as part of his PhD work. SJD and HD formulated the project and supervised the analytical work. IM oversaw the isotope analyses. KP provided ESM1, as part of her PhD thesis. BRB, SJD and HD wrote the original draft and the revised version of the manuscript.

CRediT authorship contribution statement

Brendon Rolfe-Betts: Investigation, Writing – original draft, Writing – review & editing. **Simon J. Day:** Conceptualization, Supervision, Writing – original draft, Writing – review & editing. **Hilary Downes:** Project administration, Supervision, Writing – original draft, Writing – review & editing. **Ian Millar:** Data curation, Formal analysis, Funding acquisition, Investigation. **Kristina Palubicki:** Investigation, Resources.

Declaration of competing interest

All authors declare that they have no conflict of interest.

Data availability

Data will be made available on request.

Acknowledgements

We thank Bruno Faria for logistical help, Jose Antonio Fonseca and Bob Rall for help in the field, Matthew Thirlwall and Christina Manning (Royal Holloway University of London) for access to XRF facilities, and Samantha Hammond (Open University) for the ICPMS analyses. Reviews by Abigail K Barker and Jorge E Romero were helpful in clarifying many aspects of our study. We are grateful to members of the Steering Committee of the NERC environmental isotope facility (NEIF) for access to isotope laboratories, funded by project number IP-1936-1119.

Appendix A. Supplementary data

Supplementary data to this article can be found online at https://doi.org/10.1016/j.jvolgeores.2023.107996.

References

Arai, S., 1994. Characterization of spinel peridotites by olivine-spinel compositional relationships: review and interpretation. Chem. Geol. 113 (3–4), 191–204.
Barker, A.K., Hansteen, T.H., Nilsson, D., 2019. Unravelling the crustal architecture of Cape Verde from the seamount xenolith record. Minerals 9 (2), 90.
Barker, A.K., Magnusson, E., Troll, V.R., Harris, C., Mattsson, H.B., Holm, P.M., Perez-Torrado, F.J., Carracedo, J.C., Deegan, F.M., 2023. Disequilibrium in historic volcanic rocks from Fogo, Cape Verde: Traces of carbonatite metasomatism of recycled ocean crust. Lithos 456-57, 107328.
Barrett, R., Lebas, E., Ramalho, R., Klaucke, I., Kutterolf, S., Klügel, A., Krastel, S., 2020. Revisiting the tsunamigenic volcanic flank collapse of Fogo Island in the Cape Verdes, offshore West Africa. Geol. Soc. Lond. Spec. Publ. 500, 13–26.
Bonadiman, C., Beccaluva, L., Coltorti, M., Siena, F., 2005. Kimberlite-like metasomatism and 'garnet signature'in spinel-peridotite xenoliths from Sal, Cape Verde Archipelago: relics of a subcontinental mantle domain within the Atlantic oceanic lithosphere? J. Petrol. 46 (12), 2465–2493.
Brum da Silveira, A., Serralheiro, A., Martins, I., Cruz, J., Madeira, J., Munha, J., Pena, J., Matias, L., Senos, M.L., 1995. A erupcao da Cha das Caldeiras_Ilha do Fogo. de 2 de Abril de 1995. Proteccao Civil 7, 3–14.
Brum da Silveira, A., Madeira, J., Serralheiro, A., 1997a. A estrutura da Ilha do Fogo, Cabo Verde. In: A Erupcao Vulcanica de 1995 na Ilha do Fogo, Cabo Verde. *Publ. IICT*, Lisboa, pp. 63–78.
Brum da Silveira, A., Madeira, J., Serralheiro, A., Torres, P.C., Silva, L.C., Mendes, M.H., 1997b. O controlo estrutural da erupção de Abril de 1995 na ilha do Fogo. In: A erupção vulcânica de 1995 na ilha do Fogo, Cabo Verde, pp. 51–61.
Carracedo, J.C., Day, S.J., Guillou, H., Gravestock, P., 1999. Later stages of volcanic evolution of La Palma, Canary Islands: Rift evolution, giant landslides, and the genesis of the Caldera de Taburiente. Geol. Soc. Am. Bull. 111 (5), 755–768.
Carracedo, J.C., Badiola, E.R., Guillou, H., de La Nuez, J., Torrado, F.P., 2001. Geology and volcanology of la Palma and el Hierro, western Canaries. Estudios Geologicos-Madrid 57, 175–273.
Cornu, M.N., Paris, R., Doucelance, R., Bachèlery, P., Bosq, C., Auclair, D., Benbakkar, M., Gannoun, A.M., Guillou, H., 2021. Exploring the links between volcano flank collapse and the magmatic evolution of an ocean island volcano: Fogo, Cape Verde. Sci. Rep. 11, 1–12.
Davies, G.R., Cliff, R.A., Norry, M.J., Gerlach, D.C., 1989. A combined chemical and Pb-Sr-Nd isotope study of the Azores and Cape Verde hot-spots: the geodynamic implications. Geol. Soc. Lond. Spec. Publ. 42, 231–255.
Day, S.J., Da Silva, S.H., Fonseca, J.F.B.D., 1999. A past giant lateral collapse and present-day flank instability of Fogo, Cape Verde Islands. J. Volcanol. Geotherm. Res. 94, 191–218.
Day, S.J., Carracedo, J.C., Guillou, H., Pais, F.J., Badiola, E.R., Fonseca, J.F.B.D., Heleno, S.I.N., 2000. Comparison and cross-checking of historical, archaeological and geological evidence for the location and type of historical and sub-historical eruptions of multiple-vent oceanic island volcanoes. Geol. Soc. Lond. Spec. Publ. 171, 281–306.
Deniel, C., Pin, C., 2001. Single-stage method for the simultaneous isolation of lead and strontium from silicate samples for isotopic measurements. Anal. Chim. Acta 426 (1), 95–103.
Doucelance, R., Escrig, S., Moreira, M., Gariépy, C., Kurz, M.D., 2003. Pb-Sr-he isotope and trace element geochemistry of the Cape Verde Archipelago. Geochim. Cosmochim. Acta 67, 3717–3733.
Doucelance, R., Hammouda, T., Moreira, M., Martins, J.C., 2010. Geochemical constraints on depth of origin of oceanic carbonatites: the Cape Verde case. Geochim. Cosmochim. Acta 74 (24), 7261–7282.
Escrig, S., Doucelance, R., Moreira, M., Allègre, C.J., 2005. Os isotope systematics in Fogo Island: evidence for lower continental crust fragments under the Cape Verde Southern Islands. Chem. Geol. 219, 93–113.
Farrell, J.W., Clemens, S.C., Gromet, P.L., 1995. Improved chronostratigraphic reference curve of late Neogene seawater $^{87}Sr/^{86}Sr$. Geology 23 (5), 403–406.
Foeken, J.P., Day, S., Stuart, F.M., 2009. Cosmogenic ^{3}He exposure dating of the Quaternary basalts from Fogo, Cape Verdes: implications for rift zone and magmatic reorganisation. Quat. Geochronol. 4, 37–49.
Foeken, J.P., Stuart, F.M., Mark, D.F., 2012. Long-term low latitude cosmogenic ^{3}He production rate determined from a 126 ka basalt from Fogo, Cape Verdes. Earth Planet. Sci. Lett. 359, 14–25.
Gerlach, D.C., Cliff, R.A., Davies, G.R., Norry, M., Hodgson, N., 1988. Magma sources of the Cape Verdes archipelago: isotopic and trace element constraints. Geochim. Cosmochim. Acta 52, 2979–2992.
Guillou, H., Carracedo, J.C., Day, S.J., 1998. Dating of the upper Pleistocene–Holocene volcanic activity of La Palma using the unspiked K–Ar technique. J. Volcanol. Geotherm. Res. 86 (1–4), 137–149.
Hildner, E., Klügel, A., Hauff, F., 2011. Magma storage and ascent during the 1995 eruption of Fogo, Cape Verde Archipelago. Contrib. Mineral. Petrol. 162, 751–772.
Hildner, E., Klügel, A., Hansteen, T.H., 2012. Barometry of lavas from the 1951 eruption of Fogo, Cape Verde Islands: Implications for historic and prehistoric magma plumbing systems. J. Volcanol. Geotherm. Res. 217, 73–90.
Hoernle, K., Tilton, G., Le Bas, M.J., Duggen, S., Garbe-Schönberg, D., 2002. Geochemistry of oceanic carbonatites compared with continental carbonatites: mantle recycling of oceanic crustal carbonate. Contrib. Mineral. Petrol. 142 (5), 520–542.
Holm, P.M., Wilson, J.R., Christensen, B.P., Hansen, L., Hansen, S.L., Hein, K.M., Mortensen, A.K., Pedersen, R., Plesner, S., Runge, M.K., 2006. Sampling the Cape Verde mantle plume: evolution of melt compositions on Santo Antão, Cape Verde Islands. Journal of Petrology 47 (1), 145–189.
Jackson, M.G., Becker, T.W., Konter, J.G., 2018. Evidence for a deep mantle source for EM and HIMU domains from integrated geochemical and geophysical constraints. Earth Planet. Sci. Lett. 484, 154–167.
Klügel, A., Day, S., Schmid, M., Faria, B., 2020. Magma plumbing during the 2014-2015 eruption of Fogo (Cape Verde Islands). Front. Earth Sci. 8, 157.
Kumar, A., Abouchami, W., Galer, S.J.G., Singh, S.P., Fomba, K.W., Prospero, J.M., Andreae, M.O., 2018. Seasonal radiogenic isotopic variability of the African dust outflow to the tropical Atlantic Ocean and across to the Caribbean. Earth Planet. Sci. Lett. 487, 94–105.
Le Bas, T.P., Masson, D.G., Holtom, R.T., Grevemeyer, I., 2007. Slope failures of the flanks of the southern Cape Verde Islands. In: Submarine Mass Movements and their Consequences: 3 International Symposium. Springer, Netherlands, pp. 337–345.
Lo Forte, F.M., Aiuppa, A., Rotolo, S.G., Zanon, V., 2023. Temporal evolution of the Fogo Volcano magma storage system (Cape Verde Archipelago): a fluid inclusions perspective. J. Volcanol. Geotherm. Res. 433, 107730.
Maccaferri, F., Richter, N., Walter, T.R., 2017. The effect of giant lateral collapses on magma pathways and the location of volcanism. Nat. Commun. 8, 1–11.
Machado, F., Torre de Assuncao, C.F., 1965. Carta geologica de Cabo Verde _na escala de 1/100,000.; noticia explicativa da folha da ilha do Fogo — estudos petrograficos. Garcia de Orta Lisboa. 13, 597–604.
Madeira, J., Mata, J., Mourão, C., da Silveira, A.B., Martins, S., Ramalho, R., Hoffmann, D.L., 2010. Volcano-stratigraphic and structural evolution of Brava Island

(Cape Verde) based on $^{40}Ar/^{39}Ar$, U–Th and field constraints. J. Volcanol. Geotherm. Res. 196, 219–235.
Madeira, J., Ramalho, R.S., Hoffmann, D.L., Mata, J., Moreira, M., 2020. A geological record of multiple Pleistocene tsunami inundations in an oceanic island: the case of Maio, Cape Verde. Sedimentology 67 (3), 1529–1552.
Madeira1a, J., Munhá1b, J., Tassinari, C.C.G., Mata1b, J., Martins1b, A.B.D.S.S., 2005. K/Ar ages of carbonatites from the Island of Fogo (Cape Verde). XIV semana de Geoquímica /VIII Congresso de Geoquímica dos Países de Língua Portuguesa, pp. 475–478.
Marques, F.O., Hildenbrand, A., Victória, S.S., Cunha, C., Dias, P., 2019. Caldera or flank collapse in the Fogo volcano? What age? Consequences for risk assessment in volcanic islands. J. Volcanol. Geotherm. Res. 388, 106686.
Martínez-Moreno, F.J., Santos, F.M., Madeira, J., Pous, J., Bernardo, I., Soares, A., da Silveira, A.B., 2018. Investigating collapse structures in oceanic islands using magnetotelluric surveys: the case of Fogo Island in Cape Verde. J. Volcanol. Geotherm. Res. 357, 152–162.
Masson, D.G., Le Bas, T.P., Grevemeyer, I., Weinrebe, W., 2008. Flank collapse and large-scale landsliding in the Cape Verde Islands, off West Africa. Geochem. Geophys. Geosyst. 9 (7).
Mata, J., Martins, S., Mattielli, N., Madeira, J., Faria, B., Ramalho, R.S., Silva, P., Moreira, M., Caldeira, R., Rodrigues, J., Martins, L., 2017. The 2014–15 eruption and the short-term geochemical evolution of the Fogo volcano (Cape Verde): evidence for small-scale mantle heterogeneity. Lithos 288, 91–107.
McDonough, W.F., Sun, S.S., 1995. The composition of the Earth. Chem. Geol. 120 (3–4), 223–253.
Melluso, L., Tucker, R.D., Cucciniello, C., le Roex, A.P., Morra, V., Zanetti, A., Rakotoson, R.L., 2018. The magmatic evolution and genesis of the Quaternary basanite-trachyphonolite suite of Itasy (Madagascar) as inferred by geochemistry, Sr-Nd-Pb isotopes and trace element distribution in coexisting phases. Lithos 310, 50–64.
Millet, M.A., Doucelance, R., Schiano, P., David, K., Bosq, C., 2008. Mantle plume heterogeneity versus shallow-level interactions: a case study, the São Nicolau Island, Cape Verde archipelago. J. Volcanol. Geotherm. Res. 176 (2), 265–276.
Munhá, J., Mata, J., Martins, S., Madeira, J., da Silveira, A.B., 2006. Zr/Hf, Nb/Ta and Ti/Eu fractionation in ocean island basaltic rocks: an example from Fogo Island (Cape Verde Archipelago). In: Abstract, *7th National Geological Congress of Portugal*, pp. 209–212.
Neumann, E.R., Wulff-Pedersen, E., Simonsen, S.L., Pearson, N.J., Martí, J., Mitjavila, J., 1999. Evidence for fractional crystallization of periodically refilled magma chambers in Tenerife, Canary Islands. J. Petrol. 40 (7), 1089–1123.
Paris, R., Giachetti, T., Chevalier, J., Guillou, H., Frank, N., 2011. Tsunami deposits in Santiago Island (Cape Verde archipelago) as possible evidence of a massive flank failure of Fogo's volcano. Sediment. Geol. 239, 129–145.
Pim, J., Peirce, C., Watts, A.B., Grevemeyer, I., Krabbenhöft, A., 2008. Crustal structure and origin of the Cape Verde rise. Earth Planet. Sci. Lett. 272 (1–2), 422–428.
Ramalho, R.S., Winckler, G., Madeira, J., Helffrich, G.R., Hipólito, A., Quartau, R., Adena, K., Schaefer, J.M., 2015. Hazard potential of volcanic flank collapses raised by new megatsunami evidence. Sci. Adv. 1, e1500456.
Ribeiro, O., 1960. A Ilha Do Fogo e as Suas erupções, 2nd Edn (the Island of Fogo and its Eruptions). *Memorias, Serie Geographica I*. Junta de Investigações do Ultramar, Ministério do Ultramar, Lisbon.
Ryabchikov, J.D., Ntaflos, T., Kurat, G., Kogarko, L.N., 1995. Glass-bearing xenoliths from Cape Verde: evidence for a hot rising mantle jet. Mineral. Petrol. 55, 217–237.
Shaw, C.S., Heidelbach, F., Dingwell, D.B., 2006. The origin of reaction textures in mantle peridotite xenoliths from Sal Island, Cape Verde: the case for "metasomatism" by the host lava. Contrib. Mineral. Petrol. 151 (6), 681–697.
Stillman, C.J., Furnes, H., LeBas, M.J., Robertson, A.H.F., Zielonka, J., 1982. The geological history of Maio, Cape Verde islands. J. Geol. Soc. Lond. 139, 347–361.
Thirlwall, M.F., 2002. Multicollector ICP-MS analysis of Pb isotopes using a ^{207}Pb-^{204}Pb double spike demonstrates up to 400 ppm/amu systematic errors in Tl normalization. Chem. Geol. 184 (3–4), 255–279.
Torres, P.C., Madeira, J., Silva, L.C., Brum da Silveira, A., Serralheiro, A., Mota Gomes, A., 1998. Carta Geológica das Erupções Históricas da Ilha do Fogo (Cabo Verde): revisão e actualização. Comunicações do Instituto Geológico e Mineiro 84, 193–196.
Watt, S.F., 2019. The evolution of volcanic systems following sector collapse. J. Volcanol. Geotherm. Res. 384, 280–303.
Weidendorfer, D., Schmidt, M.W., Mattsson, H.B., 2016. Fractional crystallization of Si-undersaturated alkaline magmas leading to unmixing of carbonatites on Brava Island (Cape Verde) and a general model of carbonatite genesis in alkaline magma suites. Contrib. Mineral. Petrol. 171 (5), 43.